Developmental Biology
Chromosomes and Gene Expression

Dynamic modes of Notch transcription hubs conferring memory and stochastic activation revealed by live imaging the co-activator Mastermind

F Javier deHaro-Arbona, Charalambos Roussos, Sarah Baloul, Jonathan Townson, Maria J. Gomez-Lamarca, Sarah Bray

Department of Physiology Development and Neuroscience University of Cambridge, Downing Street, Cambridge, CB2 3DY, UK • Instituto de Biomedicina de Sevilla (IBiS), Hospital Universitario Virgen del Rocío/CSIC/Universidad de Sevilla, Departamento de Biología Celular, 41013 Seville, Spain

https://en.wikipedia.org/wiki/Open_access
Copyright information

Reviewed Preprint

Revised by authors after peer review.

About eLife's process

Reviewed preprint version 2
March 20, 2024 (this version)

Reviewed preprint version 1
October 31, 2023

Sent for peer review
August 29, 2023

Posted to preprint server
August 11, 2023

Abstract

Summary

Developmental programming involves the accurate conversion of signaling levels and dynamics to transcriptional outputs. The transcriptional relay in the Notch pathway relies on nuclear complexes containing the coactivator Mastermind (Mam). By tracking these complexes in real time, we reveal that they promote formation of a dynamic transcription hub in Notch ON nuclei which concentrates key factors including the Mediator CDK module. The composition of the hub is labile and persists after Notch withdrawal conferring a memory that enables rapid reformation. Surprisingly, only a third of Notch ON hubs progress to a state with nascent transcription, that correlates with Polymerase II and core Mediator recruitment. This probability is increased by a second signal. The discovery that target-gene transcription is probabilistic has far-reaching implications because it implies that stochastic differences in Notch pathway output can arise downstream of receptor activation.

eLife assessment

This **fundamental** study advances our understanding of how Notch signaling activates transcription by analyzing dynamics of the Mastermind transcriptional co-activator and its role in the activation complex. The evidence is **compelling** and based on state of the art methods with precise quantitative measurements.

Introduction

Cells face the challenge of transmitting information accurately, so that cell-surface signals are translated into correct transcriptional responses, and how this is achieved mechanistically remains a major question. Notch is a key signalling pathway that leads to gene activation when ligand and receptor engage upon cell contact [1–3]. The physical interaction brings about a conformational change that permits proteolytic cleavage and release of Notch Intra Cellular Domain (NICD) [4–6]. This moiety forms a complex with CSL (CBF-1/RBPJ-κ in mammals, Suppressor of Hairless in *Drosophila* and LAG-1 in *C. elegans*), a transcription factor that binds to specific DNA motifs, and Mastermind (Mam) a co-activator [7–9]. This tripartite activation complex promotes transcription from the target genes where it is recruited. The sites of recruitment differ according to the cellular context, resulting in different transcriptional outcomes and suggesting that other factors are important in preparing the targets for activation [10]. In addition, release of NICD brings about rapid and robust transcriptional responses within minutes, raising the question how the molecules of cleaved Notch achieve this so efficiently [11–13].

Regulation of transcription must be tightly controlled in space, time, and genomic location [14,15]. Many different studies report that sequence-specific transcription factors, key coactivators, and RNA polymerase II (Pol II) itself undergo dynamic clustering within a nucleus [16–19]. Clustering appears to be mediated by a combination of specific structure-mediated interactions (e.g. DNA-binding, protein-protein interactions) and multivalent interactions among intrinsically disordered regions (IDRs) present in most transcription factors [20,21]. In this way, transcription is regulated by the formation of functionally specialized local protein microenvironments or transcription “hubs” associated with target enhancers [22]. In some cases, these have the properties of ‘condensates’ whose formation and dissolution has been explained by the process of phase separation [23]. As the resulting assembly is non-stoichiometric, it may enable a small number of transcription factor molecules to drive productive transcription. Such a mechanism could thus explain how NICD, whose nuclear levels are frequently below the level of detection *in vivo*, can successfully promote robust-target gene transcription [24]. Indeed, all members of the Notch activator complex contain unstructured regions that could contribute to the assembly of a hub.

The formation of the tripartite Notch activator complex involves a conserved helix in the N-terminal region of Mam proteins which is responsible for the direct interactions with CSL and NICD [8,9]. The remainder of the large Mam proteins are poorly conserved and appear to be predominantly unstructured albeit to have potential roles in recruiting other cofactors [25,26]. For example, there is evidence that human MAML1 interacts with the histone acetyl transferase CBP/p300, which is present at Notch regulated enhancers in genome-wide studies [26–28], and whose recruitment is implicated in activating some targets [29,30]. The C-terminal portion of MAML1 is also suggested to recruit CDK8, the enzymatic core of the Mediator kinase module [31–33]. What role these factors play in the recruitment, dynamics and assembly of functional Notch transcription assemblies, and whether these acquire hub-like properties is unclear.

Live imaging of endogenously tagged proteins offers a non-invasive approach to probe the assembly and composition of transcription hubs *in vivo*. Using this strategy, we have previously shown that CSL is recruited in a very dynamic manner to a target genomic locus *in vivo* [34]. However, as CSL exists in both co-repressor and co-activator complexes [35], the extent that these dynamics reflect the characteristics of the activation complex remains to be established. Here we incorporated fluorescent tags into the endogenous Mam protein to investigate the behaviours of this Notch nuclear co-activator *in vivo*, in combination with a method for live-imaging of a target genomic locus that responds robustly to Notch activation. The emerging model is that Notch activity leads to the formation of ‘transcription hubs’ that exist in different states. When Mam is present, key components of the transcriptional machinery become locally concentrated but, surprisingly, in the absence of synergising factors, the conversion to productive transcription only

occurs stochastically. In addition, the open chromatin state that is generated decays slowly after Notch withdrawal, providing a memory that enables a more rapid response to a subsequent round of Notch activation.

Results

Dynamics of Mastermind recruitment in relation to its partner CSL

The Mam co-activator is an integral part of the Notch transcription complex [8,9,30,36]. To track Mam dynamic behaviours *in vivo* we inserted GFP or Halo into the N-terminus of the endogenous Mam using CRISPR-Cas9 genome editing [34]. The resulting flies are homozygous viable with no evident phenotypes, indicating that the tagged Mam proteins are fully functional. We first set out to compare the recruitment and dynamics of CSL and Mam at a target locus in Notch OFF and Notch ON conditions, taking advantage of *Drosophila* salivary glands, where the polytene (multiple copy) chromosomes aid detection of chromatin-associated complexes. We used the Int/ParB system, where fluorescently labelled ParB proteins bind to inserted Int sequences, to detect the well-characterised *Enhancer of split complex* [*E(spl)-C*], which contains multiple Notch-regulated genes (Figure S1A, [34]). Because of the aligned copies of the genome in the polytene chromosomes, the target genomic locus appears as an easily distinguishable fluorescent “band” in each nucleus during live imaging (**Figure 1A**).

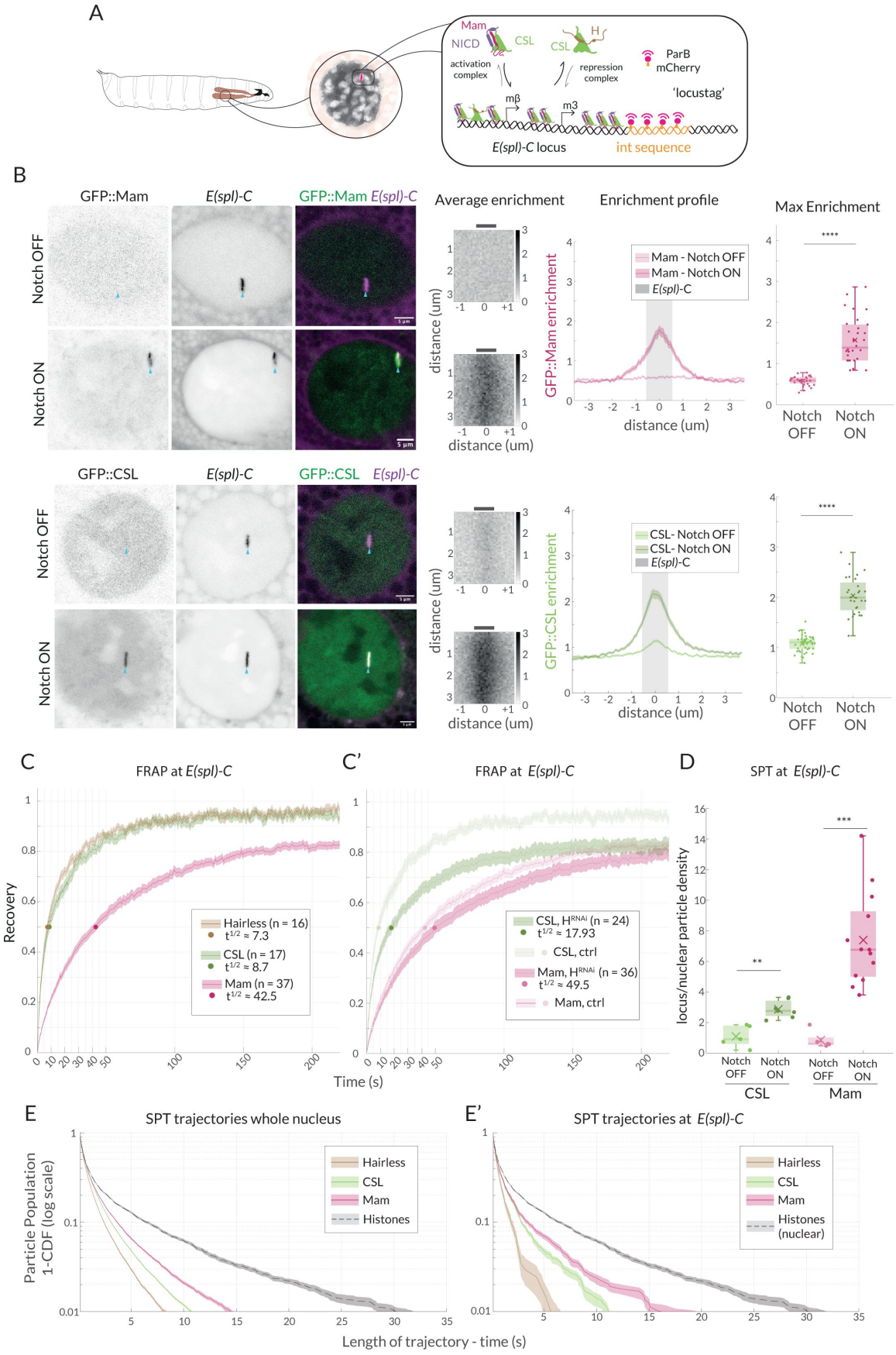
A
Mam
NICD
CSL
CSL
H
activation complex
repression complex
ParB mCherry
'locustag'
mβ
m3
E(spl)-C locus
int sequence
B
GFP::Mam
E(spl)-C
GFP::Mam E(spl)-C
Notch OFF
Notch ON
Average enrichment
Enrichment profile
Max Enrichment
distance (um)
GFP::Mam enrichment
Mam - Notch OFF
Mam - Notch ON
E(spl)-C
Notch OFF
Notch ON
GFP::CSL
E(spl)-C
GFP::CSL E(spl)-C
CSL- Notch OFF
CSL- Notch ON
GFP::CSL enrichment
C
FRAP at E(spl)-C
Recovery
Hairless (n = 16)
t1/2 ≈ 7.3
CSL (n = 17)
t1/2 ≈ 8.7
Mam (n = 37)
t1/2 ≈ 42.5
Time (s)
C'
FRAP at E(spl)-C
CSL, HRNAi (n = 24)
t1/2 ≈ 17.93
CSL, ctrl
Mam, HRNAi (n = 36)
t1/2 ≈ 49.5
Mam, ctrl
D
SPT at E(spl)-C
locus/nuclear particle density
CSL
Mam
E
SPT trajectories whole nucleus
Particle Population 1-CDF (log scale)
Hairless
CSL
Mam
Histones
Length of trajectory - time (s)
E'
SPT trajectories at E(spl)-C
Histones (nuclear)

Figure 1

Enrichment and dynamics of Mastermind at *E(spl)-C*.

(A) Schematic overview of live imaging system used. Salivary glands from *Drosophila* larvae (left) have large nuclei with polytene chromosomes (centre, grey shading) in which *E(spl)-C* locus is detected as a band (centre, red) by live imaging when labelled using Int (orange)/ParB (red) system (right and Figure S1A). Recruitment of activation complexes, [CSL (green), NICD (purple) and Mastermind (magenta)] and of co-repression complexes [CSL and Hairless (brown)] is measured by their colocalization with *E(spl)-C*.

(B) Live-imaging of GFP::Mam and GFP::CSL as indicated in relation to *E(spl)-C* marked by Int-ParB (magenta) in nuclei from Notch OFF (*1151Gal4; UAS-LacZ*) and Notch ON (*1151Gal4; UAS-NΔECD*) salivary glands. CSL and Mam are enriched at *E(spl)-C* in Notch ON but not Notch OFF cells. Average enrichment: each pixel represents average enrichment of all aligned images, centred on *E(spl)-C* locus (0, grey bar). Enrichment profile: mean enrichment, with SEM, plotted on x-axis relative to position, y axis, centred on *E(spl)-C* (0). Grey area indicates region used for max enrichment. Max enrichment: mean of 10 pixels centred on *E(spl)-C* (Figure S1B) (Mam OFF, n=32, Mam OFF, n = 30; CSL OFF, n = 45, CSL ON, n = 28, For p-values see Table S4). Box encompasses range between 0.25 and 0.75 quantile, whiskers extend to furthest points not considered outliers, bar marks median, cross marks mean and each dot is the value for one nucleus. Scale bars represent 5um. Full genotypes for all figures are provided in Table S3.

(C, C') Dynamics of CSL::GFP (green), GFP::Mam (magenta) and Hairless::GFP (brown) at *E(spl)-C* in Notch ON cells measured by FRAP. Recovery of the indicated proteins was measured in a point bleached region-of-interest centred on *E(spl)*-C and normalised by using another region and efficiency of bleaching. Dots indicate 50% recovery. Legend summarizes numbers of nuclei (n) and time to 50% recovery (t1/2). Error represents the standard error of the mean (SEM). (**C'**) FRAP analysis of CSL and Mam in cells depleted for Hairless (*1151Gal4; UAS-Hairless RNAi*) controls from C are included for comparison.

(D) Trajectory density at *E(spl)-C* relative to whole nucleus from SPT of CSL::Halo (green) and Halo::Mam (pink) in Notch OFF and Notch ON cells. Both CSL and Mam are significantly enriched in Notch ON. Box plots as in (B). CSL-OFF, n = 5, CSL-OFF, n = 7; Mam-OFF, n = 5, Mam-ON, n = 13; For number of trajectories see Figure S1F and for p-values see Table S4.

(E, E') Survival curves depicting duration of trajectories in SPT of the indicated Halo fusion proteins in whole nuclei (E) and at *E(spl)-C* (E'), in Notch ON cells. Whole nuclei H2B::Halo trajectories are included for comparison in both graphs. For number of trajectories, see Figure S1F. Error bars represent 95% confidence intervals, obtained from bootstrapping with 100 resampled datasets [103].

The Notch pathway is normally inactive in salivary glands, providing a baseline Notch OFF condition. This was converted to Notch ON by the expression of a constitutively active form of Notch, NΔECD, using the GAL4-UAS system which allows tissue-specific and temporal control. Because it lacks the extracellular domain, NΔECD is constitutively cleaved by gamma-secretase to release NICD, mimicking ligand induced activation [37–39]. Comparing the localization of GFP::Mam in Notch OFF and Notch ON conditions, it was immediately evident that Mam was robustly recruited to *E(spl)-C* in Notch ON conditions in a similar manner to CSL [34]. In Notch OFF conditions, both proteins were diffuse throughout the nucleus, with a low level of CSL, but not Mam, present at *E(spl)-C*. In Notch ON conditions, strong enrichment of both Mam and CSL was consistently detected around *E(spl)-C*, where the two proteins co-localise in a correlated manner (**Figure 1B**, S1C).

To compare the dynamics of Mam and CSL at *E(spl)-C* in Notch ON conditions, we performed Fluorescence Recovery After Photobleaching (FRAP) focussed on the region defined by the locus-tag. Unlike CSL, which had a rapid recovery ($t_{1/2}$=9 secs), Mam exhibited slower dynamics

($t_{1/2}$=40 secs) and failed to fully recover over the time-course of the experiment (**Figure 1C**). Slower recovery can arise from higher proportion of bound molecules, longer residence times and/or slower diffusion coefficients[40]. The results therefore suggest that the Mam-containing activation complexes have different properties from the majority of CSL complexes.

The other main partner for CSL in *Drosophila* is the co-repressor Hairless. In FRAP experiments Hairless has a fast recovery, with a profile close to that of CSL (**Figure 1C**), consistent with a significant fraction of CSL being complexed with Hairless even in Notch ON conditions[34]. The difference in dynamics between CSL and Mam could therefore be explained by the former being involved in two different complexes with different dynamics. To test this, we depleted Hairless using RNAi-mediated knock-down, which we validated by RT-qPCR, and measured the effects on enrichment and dynamics of CSL and Mam (Fig. S1D). As expected, Mam recruitment levels and the dynamics measured by FRAP were unchanged (**Figure 1C'**, S1E). In contrast, CSL levels and recruitment were reduced and its FRAP recovery was slowed, albeit not to the extent that it recapitulated the Mam profile (**Figure 1C'**, S1E). Together the results indicate that the activation complexes, containing CSL and Mam, have slower dynamics than the repressor complexes, containing CSL and Hairless, and that the recovery of CSL reflects its participation in the two types of complexes.

To further investigate the dynamics of Mam and CSL complexes, we performed single particle tracking (SPT) by sparse labelling of endogenous Halo::Mam and Halo::CSL in live tissue [41,42]. Gaussian fitting-based localisation and multiple hypothesis tracking were used for detection and tracking of single particles within the nucleus with a ~20nm precision[34]. Using a Bayesian treatment of Hidden Markov Models, vbSPT [43], trajectories were assigned into 2 states, defined by a Brownian motion diffusion coefficient, that correspond to "bound" chromatin associated molecules (diffusion coefficient 0.01μm^2/s) versus more freely diffusing complexes (diffusion coefficient >0.25μm^2/s). A greater proportion (55%) of Mam complexes were in the bound state than CSL complexes (39%), consistent with the differences between their FRAP curves (Figure S1F). We also analysed the density of particle trajectories in relation to the *E(spl)-C* locus in Notch OFF and Notch ON conditions. In comparison to their average distribution across the nucleus, both CSL and Mam trajectories were significantly enriched in a region of approximately 0.5 μm around the target locus in Notch ON conditions, reflecting robust Notch dependant recruitment to this gene complex (**Figure 1D**).

To assess whether Mam complexes have longer residence times once recruited to the chromatin, we analysed the duration of trajectories for Mam, CSL and Hairless. Long trajectories correlate to bound complexes, because faster moving particles are rapidly lost from the field of view, and the length of time they are detectable is an indication of relative residence times. There were clear differences between the trajectory durations for Mam, CSL and Hairless. Mam trajectories had the longest durations of up to 15 secs, Hairless trajectories were the shortest (up to 5-7 secs) and CSL trajectories were intermediate (up to 10 secs) (**Figure 1E**). The differences were recapitulated when only the trajectories in the region around *E(spl)-C* were analysed (**Figure 1E'**). The residences are likely an underestimation because bleaching and other technical limitations also affect the track durations[44]. Nevertheless, these data confirm that Mam-containing complexes have on average longer residence times than other CSL complexes which, together with the higher proportion of bound molecules overall, explains the slower recovery dynamics measured by FRAP.

The fact that CSL dynamics, measured by FRAP and SPT, are intermediate between Hairless and Mam fit well with it being present in two types of complexes [co-activator (Mam) and co-repressor (Hairless)]. However, whether the contribution from CSL co-repressor complexes can fully explain all the observed differences between CSL and Mam is not fully clear. First, when we depleted Hairless, so that the majority of CSL present would be in co-activator complexes, CSL FRAP recovery curves were still substantially different from those of Mam. Second, none of the CSL trajectories had a duration approximating those of the longest-lasting Mam trajectories, despite

that over 50,000 CSL trajectories were tracked (compared to 14,000 Mam, Figure S1F). It is possible therefore that, once recruited, Mam can be retained at target loci independently of CSL by interactions with other factors so that it resides for longer.

Hub-like properties of CSL-Mastermind complexes in Notch active cells

The enrichment of CSL and Mam around *E(spl)-C* that we detect by live-imaging is not unexpected because this locus has multiple genes containing CSL binding-motifs [34,45]. However, the diffuse enrichment was not maintained when the tissues were fixed, a characteristic reported for proteins present in condensate-like hubs [46] (Figure S2A). The localized concentration of exchanging CSL and Mam complexes around *E(spl)-C* in Notch ON nuclei may therefore have properties of a transcription hub, with some of the recruitment being reliant on weak interactions mediated by low-complexity regions [47–49].

First, we asked to what extent CSL recruitment was correlated with the number of CSL binding motifs. To do so, we took advantage of fly strains containing multiple copies of CSL motifs inserted at an ectopic position in the genome [50] and compared the recruitment with insertions containing 12 or 48 CSL motifs. In Notch ON conditions, these insertions were sufficient to generate an ectopic band of CSL recruitment similar to the native *E(spl)-C* (**Figure 2A**). Remarkably the amounts of CSL recruited to loci with 12 and 48 ectopic sites were almost identical. Thus, there is not a direct correlation between the number of motifs and the amount of CSL recruited under these conditions, although we note that DNA binding is a pre-requisite as no recruitment occurs with CSL mutant that lacks DNA binding [34]. Nor does it appear that the amounts of CSL complexes are a limiting factor as there was no decrease in recruitment at the endogenous *E(spl)*-C locus, even in nuclei with a 48 CSL-motif insertion.

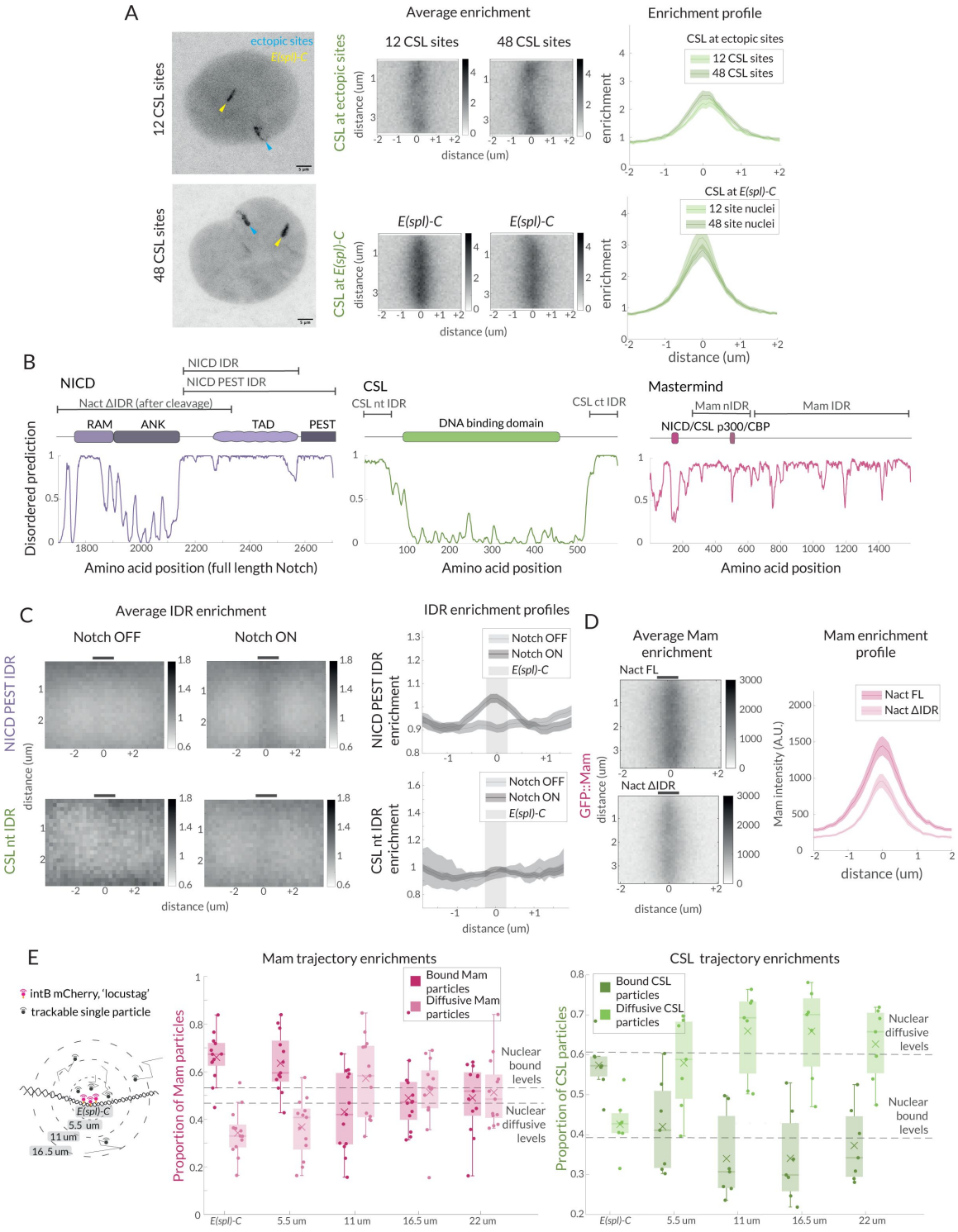
A
Average enrichment
Enrichment profile
12 CSL sites
48 CSL sites
ectopic sites
E(spl)-C
CSL at ectopic sites
CSL at E(spl)-C
distance (um)
enrichment
CSL at ectopic sites
12 CSL sites
48 CSL sites
CSL at E(spl)-C
12 site nuclei
48 site nuclei
B
NICD
NICD IDR
NICD PEST IDR
Nact ΔIDR (after cleavage)
RAM
ANK
TAD
PEST
Disordered prediction
Amino acid position (full length Notch)
CSL
CSL nt IDR
CSL ct IDR
DNA binding domain
Amino acid position
Mastermind
Mam nIDR
Mam IDR
NICD/CSL p300/CBP
Amino acid position
C
Average IDR enrichment
IDR enrichment profiles
Notch OFF
Notch ON
E(spl)-C
NICD PEST IDR
CSL nt IDR
distance (um)
NICD PEST IDR enrichment
CSL nt IDR enrichment
D
Average Mam enrichment
Mam enrichment profile
Nact FL
Nact ΔIDR
GFP::Mam
Mam intensity (A.U.)
distance (um)
E
intB mCherry, 'locustag'
trackable single particle
E(spl)-C
5.5 um
11 um
16.5 um
Mam trajectory enrichments
Bound Mam particles
Diffusive Mam particles
Proportion of Mam particles
Nuclear bound levels
Nuclear diffusive levels
CSL trajectory enrichments
Bound CSL particles
Diffusive CSL particles
Proportion of CSL particles
22 um

Figure 2

Hub-like properties of recruited complexes in Notch ON nuclei.

(A) Representative images of GFP::CSL in Notch ON nuclei containing an ectopic array of 12 or 48 CSL binding sites. GFP::CSL is recruited to *E(spl)-C* (yellow) and the ectopic array (blue). Average enrichment, Enrichment profile as in **Figure 1B**; (ectopic array 12, n=45, ectopic array 48, n = 40; *E(spl)-C* 12, n=45, *E(spl)-C* 48, n=40).

(B) Domain organisation of the indicated proteins is diagrammed above the prediction scores (Metapredict V2) of protein disorder for each. Regions tested as IDRs are indicated.

(C) Average enrichments and enrichment profiles of NICD-PEST IDR (Notch OFF, n = 62, Notch ON, n = 67) and CSL-nt IDR (Wilcoxon rank sum test: Notch OFF, n = 8, Notch ON, n = 40) at *E(spl)-C* in Notch OFF and Notch ON cells.

(D) Average enrichments and enrichment profiles (as in **Figure 1B**) of GFP::Mam at *E(spl)-C* in nuclei expressing intact (Nact) and IDR deleted (Nact ΔIDR) Notch constructs (Nact, n = 58, Nact ΔIDR, n = 55). p-values in Table S4

(E) Diagram illustrates concentric ring analysis of single particle trajectories at increasing distances from *E(spl)-C*. Graphs plot proportions of bound (dark shading) and diffusive (light shading) particles of Halo::Mam or Halo::CSL within each ring. Dashed lines indicate nuclear proportions of each population as indicated. For number of trajectories see Figure S1F.

See also Supplementary Figure S2.

Second, we questioned whether the non-stochiometric recruitment of activator complexes to loci with CSL motifs might involve additional weak protein-protein interactions between some components, as observed in several transcription hubs where intrinsically disordered protein domains play a part [20,51]. We used Intrinsically Disordered Region (IDR) prediction algorithms [52] to identify IDRs within NICD, CSL, Mam and Mediator1 (Med1, part of the mediator complex) (**Figure 2B**) and generated transgenic flies where each IDR was expressed as a fusion with GFP. The recruitment of the IDR::GFP fusions to *E(spl)-C* was then measured in Notch ON and OFF conditions (**Figure 2C**). Of the IDRs tested, the C-terminal region from NICD was the most strongly enriched at *E(spl)-C* in Notch ON conditions. A low level of enrichment was also evident for a shorter NICD fragment, that lacked the C-terminal PEST sequences and for Med 1 IDR but not for the terminal regions of CSL. Surprisingly, little or no enrichment occurred with Mam-IDRs, despite that this large protein has been reported to interact with p300 and other factors (Figure S2C) and that the mammalian MamL1 forms puncta when over expressed [53]. Notably however, Mam-nIDR::GFP fusion was present in droplets, suggesting it can self-associate when present in a high local concentration (Figure S2B, [54]). Our results suggest therefore that the IDR in NICD may contribute to the localized enrichments at target loci in Notch ON cells, potentially in combination with IDRs present in other recruited factors. In support of this hypothesis, deletion of the IDR from NICD led to a reduction in the levels and stability of Mam recruitment to *E(spl)-C* (**Figure 2D**).

Third, we reasoned that the presence of a transcription hub, where complexes are retained in the vicinity via protein interactions, should result in local changes in the behaviours of CSL and Mam. After segregating the SPT trajectories according to their diffusion properties as described above (Figure S1F), we analysed the spatial distribution of the slow and fast populations in relation to the *E(spl)-C,* defined as the area within 550nm of the locus-tag. Based on the shape and centre of this region, concentric zones were defined at 550nm distances and the proportions of slow- and fast-moving particles in each zone were calculated. The results show that there is an enrichment for slow-diffusing and a depletion of fast-moving particles close to the locus, with these altered properties extending to a region of up to 1μm away (**Figure 2E**).

Together our data support the model that CSL-Mam complexes are recruited and form a hub of high protein concentrations around the target locus in Notch ON conditions and suggest that IDR interactions, as well as DNA binding, contribute to their recruitment and retention in a region surrounding the active enhancers.

Mediator CDK module is required for stable Mastermind recruitment

The hub-like properties and slower turnover of Mam complexes compared to CSL suggest that other factors will be involved in their stabilization. We therefore tested the consequences of inhibiting or depleting different factors to distinguish those required for Mam enrichment at *E(spl)-C* in Notch ON nuclei. We first asked whether active transcription was required for Mam recruitment, by exposing the tissue to triptolide, a fast and specific inhibitor of transcription initiation which effectively inhibited transcription in Notch ON cells (Figure S3A, [55]). No change in Mam enrichment or recovery was detected, arguing that Mam recruitment is not dependent on initiation or RNA production (**Figure 3A**, B). As previous studies have reported an interaction between Mam and the histone acetylase CBP/p300 [30,33,56,57], we next inhibited CBP activity using a potent and selective inhibitor A485 [58]. Tissues were exposed to A485 for one hour which was sufficient to severely reduce the levels of H3K27Ac and *E(spl)*m3 transcription, indicating that the treatment was effective (Figure S3B-C). Surprisingly however, there was no change in the recruitment of Mam in these conditions (**Figure 3C**). We also depleted CBP by RNAi and, as with the drug treatment, Mam recruitment was unchanged (**Figure 3D**, S3J). Based on these results, we conclude that CBP is not essential for the recruitment of Mam complexes to the hub formed at the *E(spl)-C*C locus.

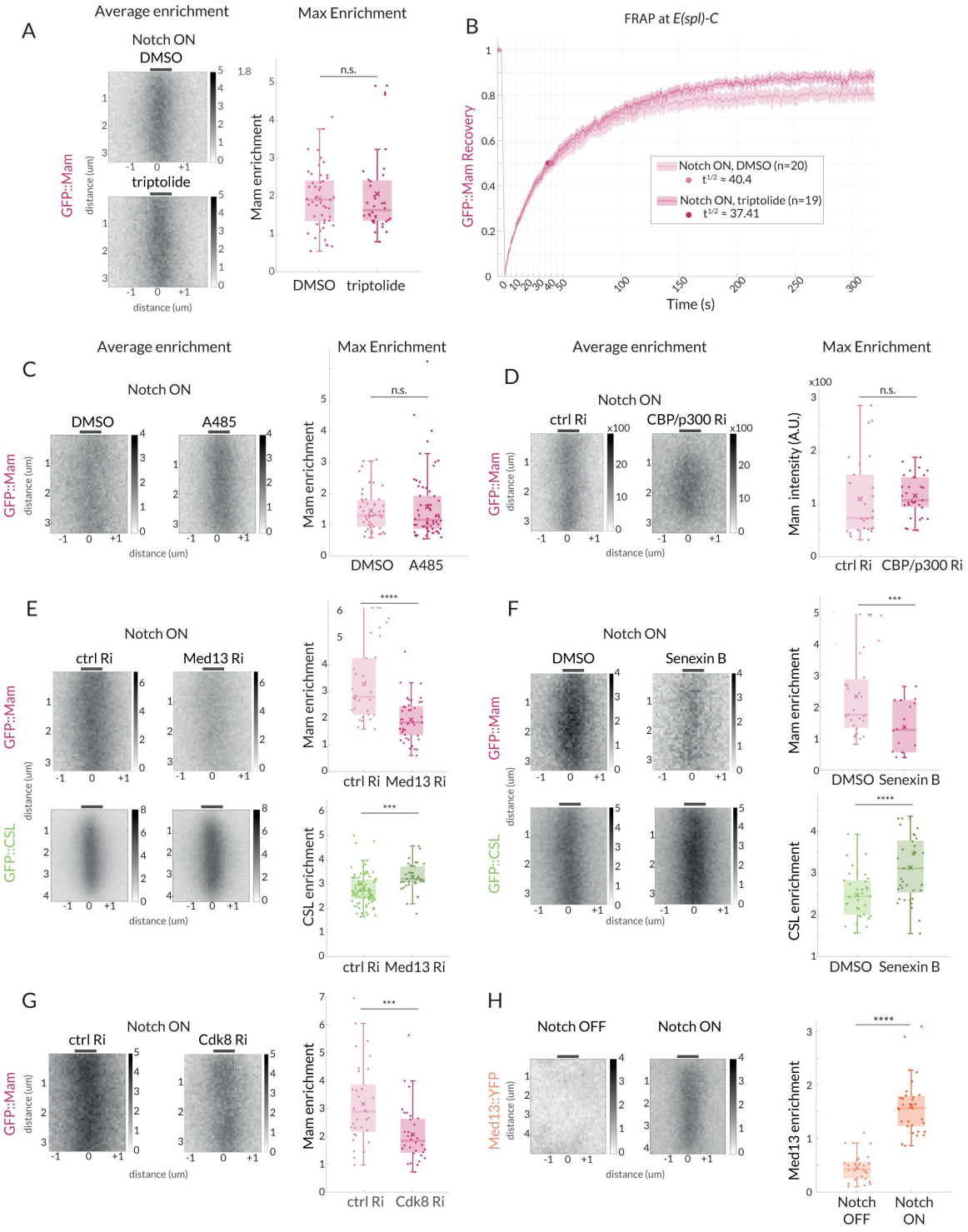
A
Average enrichment
Notch ON
DMSO
triptolide
GFP::Mam
distance (um)
Max Enrichment
Mam enrichment
n.s.
DMSO triptolide
B
FRAP at E(spl)-C
GFP::Mam Recovery
Notch ON, DMSO (n=20)
t1/2 ≈ 40.4
Notch ON, triptolide (n=19)
t1/2 ≈ 37.41
Time (s)
C
Average enrichment
Notch ON
DMSO
A485
Max Enrichment
n.s.
DMSO A485
D
Average enrichment
Notch ON
ctrl Ri
CBP/p300 Ri
x100
Max Enrichment
Mam intensity (A.U.)
n.s.
ctrl Ri CBP/p300 Ri
E
Notch ON
ctrl Ri
Med13 Ri
GFP::CSL
CSL enrichment
****
***
ctrl Ri Med13 Ri
F
Notch ON
DMSO
Senexin B
DMSO Senexin B
G
Notch ON
ctrl Ri
Cdk8 Ri
ctrl Ri Cdk8 Ri
H
Notch OFF
Notch ON
Med13::YFP
Med13 enrichment
Notch OFF
Notch ON

Figure 3

Mam enrichment requires Mediator CDK module but is independent of transcription and CBP/p300.

(A-B) GFP::Mam recruitment levels and dynamics at *E(spl)-C* in Notch ON tissues treated with triptolide or DMSO as a control. (A) Average and Max enrichment as in **Figure 1B**, (DMSO n = 49, triptolide, n = 36). (B) FRAP recovery curves, plotted as in **Figure 1C**.

(C–F) Average enrichment and Max enrichment of GFP::Mam and GFP::CSL, as indicated, at *E(spl)-C* in Notch ON control and treated tissues**. (C-D)** No change in recruitment following inhibition (C, A485) or genetic knockdown (D, RNAi) of CBP/p300 compared to control, DMSO and *yellow* RNAi (yRi) respectively. (DMSO, n = 47, A485, n = 62; *y* RNAi, n = 26, CBP/p300 RNAi, n = 31). **(E, F)** Reduced recruitment of GFP::Mam (magenta) but not CSL::GFP (green) following (E) genetic knockdown of Med13 and (F) inhibition of CDK8 with Senexin B. (E: Mam control, n = 30, Mam Med13Ri, n = 45; CSL control, n=92, CSL Med13Ri, n = 36) and (F: Mam ctrl n = 27, Mam Senexin, n = 43; CSL ctrl, n = 34, CSL Senexin, n = 37).

(G) Genetic knockdown of Cdk8 results in decreased Mam recruitment compared to controls (ctrl, n=33, Cdk8 Ri, n = 32). Box plots in A-F as in **Figure 1B**. For p-values see Table S4.

(H) Average enrichment and max enrichment of Med13::YFP at *E(spl)-C* in Notch OFF, n = 28 and Notch ON, n = 31; For p-values see Table S4.

See also Supplementary Figure S3.

As several studies have suggested that the Mediator CDK module, containing Med12, Med 13, CDK8 and CycC, influences Notch dependent transcription, we next focused on the role of this complex [31,32,59]. First, we depleted Med13 and CDK8 using well validated RNAi lines ([60,61], S3J). Med13 depletion led to a loss of *E(spl)*m3 transcription, confirming its role (Figure S3E). In these conditions we detected a substantial reduction in Mam recruitment to *E(spl)-C* in Notch ON cells, suggesting the CDK module plays a role in retaining Mam at target sites (**Figure 3E**, G). Second, we incubated the tissues in Senexin B or Senexin A, two drugs that target CDK8 activity [62,63] for 1 hour prior to imaging. In both cases the treatment was sufficient to significantly impair Mam levels at *E(spl)*-C (**Figure 3F**, S3D) while a CDK9 inhibitor, NVP2, had no effect in the same assays despite a loss of *E(spl)*m3 transcription (Figure S3H-I). We note that human MamL1 is a high confidence CDK8 target [64], but as the phospho-sites are not conserved it is unclear whether Mam would also be a direct target of the kinase. Third we investigated whether CDK module was recruited to *E(spl)-C*, in Notch ON nuclei using an existing line in which YFP is fused to Med13 [65,66]. Significant enrichment of Med13::YFP was detected at *E(spl)-C* in Notch ON nuclei, (**Figure 3H**) demonstrating that it is present in the hub with Mam.

Despite their effects on Mam recruitment, neither depletion of Med13 nor Senexin treatments caused any significant reduction in the levels of CSL recruited. On the contrary, a small increase occurred (**Figure 3E**, F). One explanation for the differences in the effects on CSL and Mam could be that there is increased recruitment of CSL complexes containing the co-repressor, Hairless, following Senexin treatment. We therefore monitored Hairless recruitment under these conditions but detected no increase in Senexin treated nuclei (Figure S3F). However, the overall nuclear levels of Hairless are quite high making it difficult to detect and quantify any changes at *E(spl)-C*. We therefore investigated the impact of Senexin on recruitment of a mutant CSL (CSL-Hmut) with compromised Hairless binding. This retains normal recruitment in control Notch ON conditions (Figure S3G) but, strikingly, it is not enriched at *E(spl)-C* in Senexin treated tissues. This result suggests that CSL requires Hairless interaction for its recruitment to *E(spl)-C* upon CDK8

inhibition. The differences in the effects on Mam and CSL imply that the CDK module is specifically involved in retaining Mam in the hub, and that in its absence other CSL complexes containing Hairless “win-out”, either because the altered conditions favour them and/or because they are the more abundant.

Mastermind is not essential for chromatin accessibility

The observed differences between CSL and Mam in their dynamics and dependency on the CDK module led us to speculate that they make different functional contributions to the transcription hub. To probe the role of Mam, we examined the consequences when its recruitment to the complex was prevented. The N-terminal peptide from Mam functions as a dominant negative (MamDN) by occupying the groove formed by CSL-NICD and, when overexpressed, prevents transcription of target genes [8,9,67]. As predicted, MamDN expression in Notch ON conditions prevented recruitment of full-length Mam to *E(spl)*-C (**Figure 4A**). To verify that MamDN also inhibited transcription under these conditions, we used single molecule Fluorescent in situ hybridization (smFISH) with probes targeting *E(spl)-C* transcripts that are robustly up-regulated in this tissue [34]. Nascent transcripts of *E(spl)*m3 were detected at *E(spl)*-C in Notch ON nuclei and were at very reduced levels in nuclei co-expressing MamDN (**Figure 4D**, D’) confirming that target-gene transcription is blocked.

By contrast, recruitment of CSL was unaffected by MamDN expression. It was robustly recruited to *E(spl)*-C at a similar level to untreated Notch ON nuclei despite the absence of full-length Mam (**Figure 4A**’, [34]). Identical results were obtained when Mam was depleted by RNAi (Figure S4A, [34]). The fact that CSL was still strongly enriched under these conditions argues that some of the Notch induced changes at *E(spl)-C* occur independently of the co-activator, as proposed previously [34]. In contrast to CSL, the enrichment of Med13 was lost in the presence of MamDN revealing that Med13 recruitment requires Mam, as well as the converse (**Figure 4C**).

Since MamDN does not prevent CSL recruitment, although it blocks recruitment of Med13 and transcription, we hypothesised that some Notch-induced effects at target enhancers may not require Mam. One consequence from Notch activation is an increase in chromatin accessibility at sites where CSL is recruited [34,68]. We therefore asked whether changes in chromatin accessibility still occur in the presence of MamDN by performing ATAC and analysing by qPCR the accessibility of the regulatory regions abutting *E(spl)*mβ and *E(spl)*m3 [34]. Both regions significantly increased in accessibility in Notch ON nuclei which was maintained in the presence of MamDN (**Figure 4B**). In addition, we found that the levels of GFP::NICD-IDR recruited to *E(spl)*-C were similar in the presence and absence of MamDN (Figure S4B), arguing that a modified hub is still formed.

Altogether these observations support the model that the increased chromatin accessibility elicited by Notch activation can occur independently of Mam and must rely on other functions conferred by CSL and NICD [34], while Mam is essential to recruit the Mediator CDK module and enable transcription.

CSL recruitment and chromatin accessibility persist after Notch inactivation, conferring memory

Our results suggest that there are two or more separable steps involved in forming an active transcription hub in Notch ON cells: a Mam-independent change in chromatin accessibility, a Mam-dependent recruitment of Mediator and initiation of transcription. If these are discrete steps, we reasoned that they might decay with different kinetics when Notch activity is removed. We took advantage of the thermosensitive Gal4/Gal80ts system to switch off Notch activity and assessed the consequences on CSL and Mam recruitment at two different time points: 4 hours and 8 hours after the switch-off. Imaging Mam::GFP and CSL::mCherry simultaneously, it was evident that Mam recruitment levels decreased more rapidly. CSL remained relatively constant through

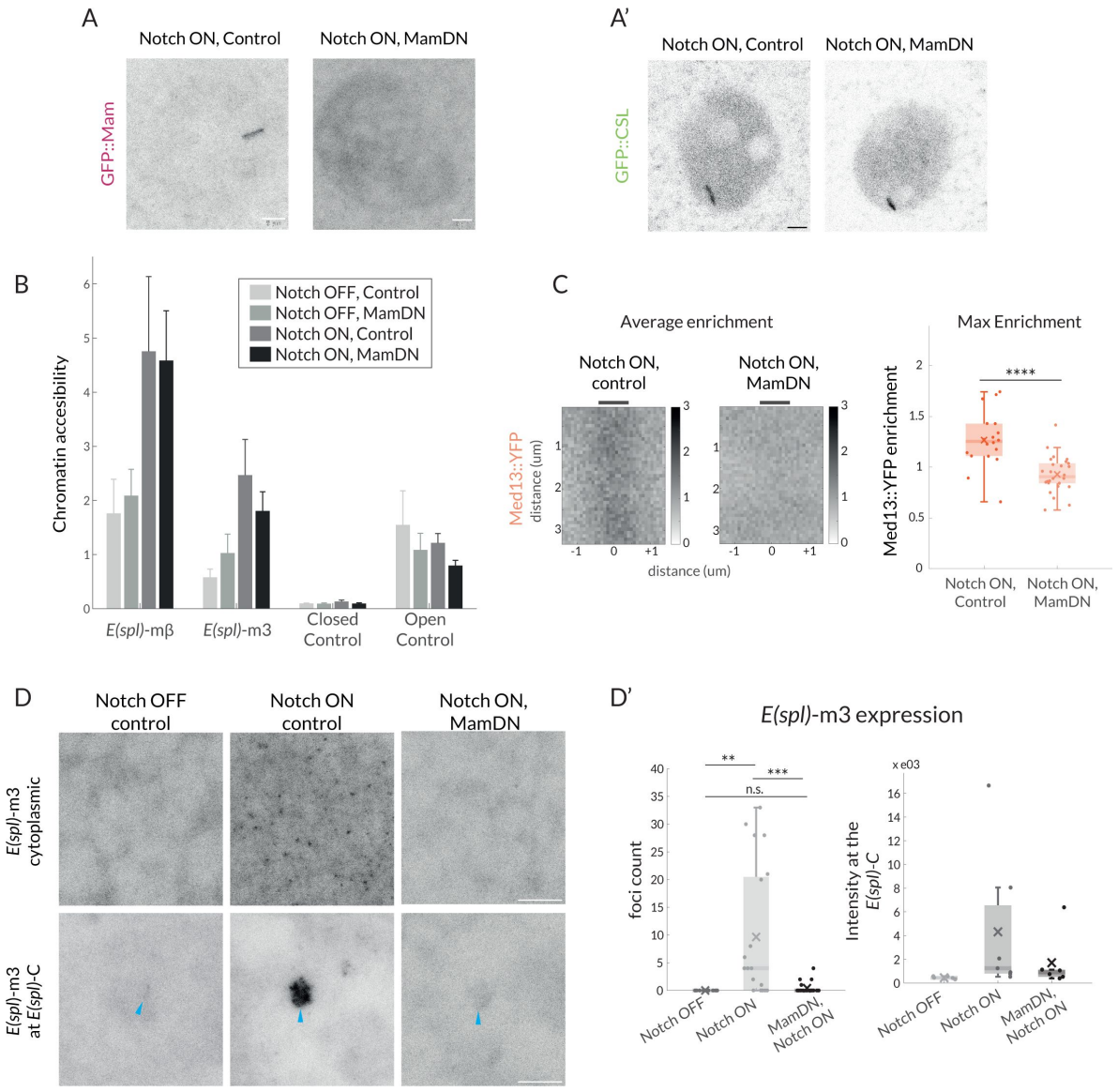

Figure 4

Mam is not necessary for CSL enrichment and chromatin opening but necessary for transcription and Mediator 13 enrichment.

(A-A') Recruitment of GFP::Mam in Notch ON nuclei is perturbed by MamDN (*1151-Gal4 UAS-MamDN*) (A) while recruitment of GFP::CSL is unaffected (A'). Control UAS was included in Notch ON combinations, details of genotypes are provided in Table S3. Scale bars represent 5um.
(B-B') Accessibility of Notch regulated enhancers adjacent to *E(spl)* -mβ and *E(spl)* -m3 under the conditions indicated was probed using ATAC-qPCR. Values were normalised to Rab11, error bars represent SEM. Closed control is a noncoding genomic region in chromosome 3 and open control' Eip78, an ecdysone responsive region active in L3 larval stage.
(C) Average enrichment and max enrichment of Med13::YFP at *E(spl)-C* in Notch ON conditions only, and in combination with MamDN. Quantifications as in **Figure 1B**, OFF, n=28, ON, n = 31. For p-values see Table S4
(D-D') Expression of *E(spl)*-m3, detected by smFISH in the conditions indicated; representative images from cytoplasm (upper; 1.8mm^3) and nucleus (lower; centred on *E(spl)-C*, blue arrows). Scale bars represent 5um. Graphs (D'), number of RNA puncta (cytoplasmic, n = 18, 20 and 22) and locus intensity (nucleus, n = 6, 7 and 6) in Notch OFF, Notch ON ctrl and Notch ON MamDN as indicated, boxplots as described in **Figure 1B**.
See also Supplementary Figure S4.

both time points while, in contrast, the levels of Mam at *E(spl)-C* decreased sharply after 4 hours (**Figure 5A**). Based on these results we propose that, after Notch activity decays, the locus remains accessible because when Mam-containing complexes are lost they are replaced by other CSL complexes (e.g. co-repressor complexes).

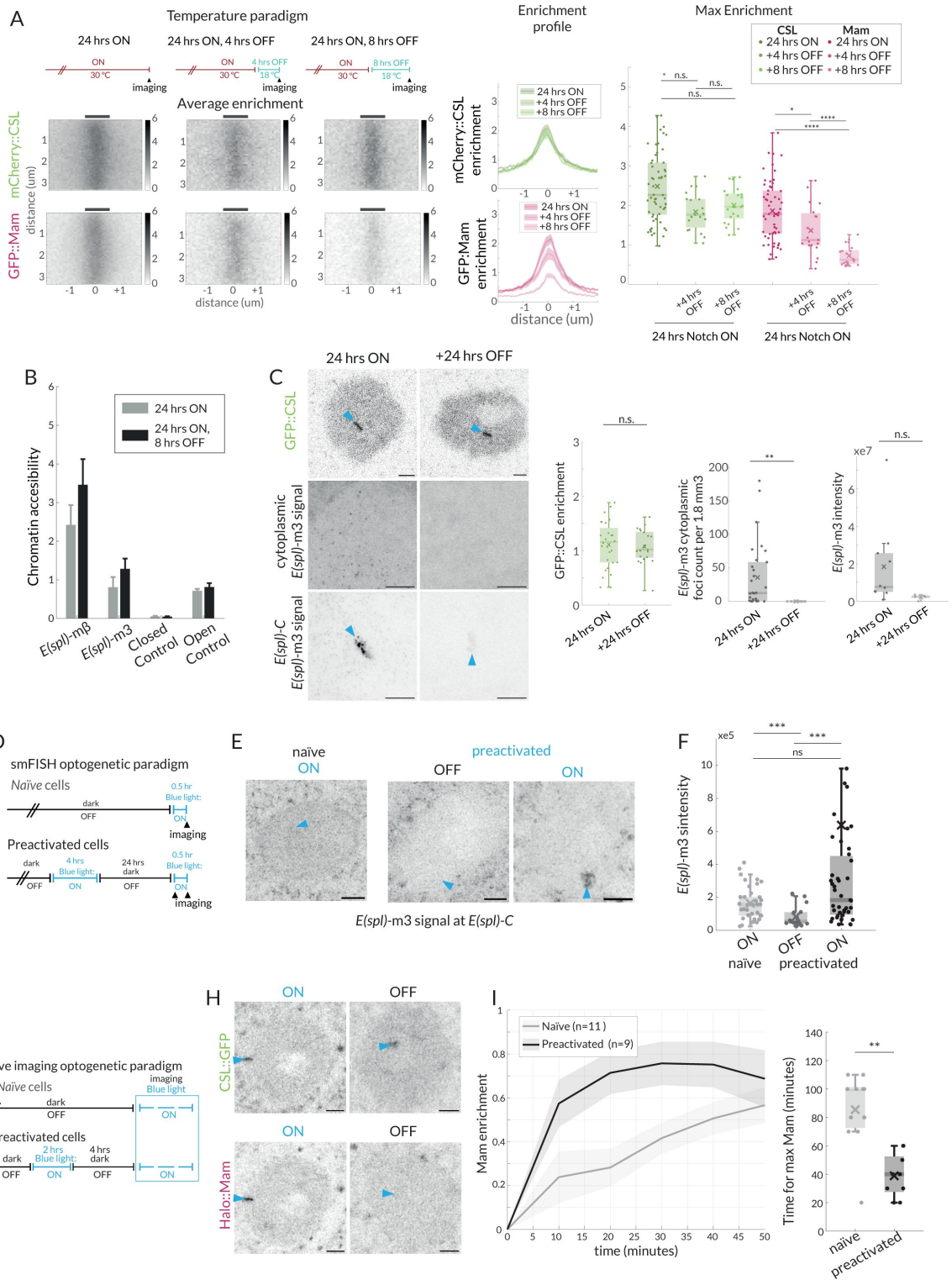
A
Temperature paradigm
24 hrs ON
24 hrs ON, 4 hrs OFF
24 hrs ON, 8 hrs OFF
imaging
Average enrichment
mCherry::CSL
GFP::Mam
distance (um)
Enrichment profile
24 hrs ON
+4 hrs OFF
+8 hrs OFF
Max Enrichment
CSL
Mam
n.s.
24 hrs Notch ON
B
Chromatin accesibility
E(spl)-mβ
E(spl)-m3
Closed Control
Open Control
C
24 hrs ON
+24 hrs OFF
GFP::CSL
cytoplasmic E(spl)-m3 signal
E(spl)-C E(spl)-m3 signal
GFP::CSL enrichment
E(spl)-m3 cytoplasmic foci count per 1.8 mm3
E(spl)-m3 intensity
D
smFISH optogenetic paradigm
Naïve cells
Preactivated cells
dark
OFF
Blue light:
ON
E
naïve
preactivated
E(spl)-m3 signal at E(spl)-C
F
E(spl)-m3 sintensity
naïve
preactivated
G
Live imaging optogenetic paradigm
Naïve cells
Preactivated cells
H
CSL::GFP
Halo::Mam
I
Naïve (n=11)
Preactivated (n=9)
Mam enrichment
time (minutes)
Time for max Mam (minutes)

Figure 5

Effects of Notch withdrawal on hub composition imply memory state.

(A) Temperature paradigm: Withdrawal of Notch activity using the thermosensitive Gal4/Gal80ts system; after a 24h ON period, larvae were transferred to 18C (Gal4 inhibited) for the indicated periods (top) and enrichment of mCherry::CSL and GFP::Mam at *E(spl)-C* imaged. Average enrichment, enrichment profiles and max enrichment quantified as in **Figure 1B**. 24 hrs ON, n = 28, 24 hrs ON, 4 hrs OFF, n = 21, 24 hrs ON, 8 hrs OFF, n = 19. p-values are summarized in Table S4.

(B) Accessibility of enhancers at *E(spl)* -mβ and *E(spl)* -m3, in Notch ON and after Notch withdrawal (8 hours) was probed using ATAC-qPCR, as in **Figure 4B**.

(C) Recruitment of CSL::GFP and expression of *E(spl)*-m3, detected by smFISH in the conditions indicated. Robust recruitment of CSL::GFP at E(spl)-C persists after switching to none-permissive temperature (Notch OFF) for 24hours, representative image and graph (green) with intensity quantifications for multiple nuclei (24 hrs ON, n = 28, + 24 hrs OFF, n = 21). For smFISH, representative images from cytoplasm (upper; 1.8 mm^3) and nucleus (lower; centred on *E(spl)-C, blue* arrow), are shown, scale bars represent 5um. RNA puncta are absent after 24 hours Notch OFF. Graphs show number of cytoplasmic RNA puncta (left) from n = 30, 16 regions and RNA fluorescence intensity at *E(spl)*-C in the conditions indicated from n = 10, 5 nuclei, with boxplots as described before (**Figure 1B**). p-values in Table S4.

(D) Optogenetic paradigm used for smFISH: Conditions used to switch ON and OFF Notch activity using

OptiC Notch [69].

(E-F) Expression of *E(spl)*-m3, detected by smFISH in the conditions indicated. (E) Representative images from the nucleus (centred on *E(spl)-C*, blue arrows). Scale bars represent 5um. (F) Graphs for fluorescence intensity at *E(spl)*-C in the conditions indicated from n = 38, 21 and 43 nuclei, with boxplots as described before (**Figure 1B**). p-values in Table S4.

(G) Optogenetic paradigm used for live imaging: Conditions used to switch ON and OFF Notch activity using OptiC Notch [69].

(H) Recruitment of CSL::GFP and Mam::Halo at *E(spl)-C*, measured following blue light activation in OptiC Notch expressing tissues for 2 hours (ON) and after 4 hours in dark (OFF). GFP::CSL remains enriched, Halo::Mam is depleted.

(I). Recruitment of Halo::Mam in preactivated nuclei compared to naïve nuclei; temporal profile of Mam::Halo enrichment (right) and time taken to max enrichment (left). Error bars in the profile represents the SEM, values were normalised from 0 to 1 (similar to FRAP recovery, see **Figure 1** and methods), n indicates the number of nuclei from >3 salivary glands. Boxplots parameters as in **Figure 1B**; naïve, n = 11, preactivated n = 9.

As Notch removal leads to a loss of Mam, but not CSL, from the hub, we hypothesised it would recapitulate the effects of MamDN on chromatin accessibility and transcription of targets. We therefore measured the accessibility of target enhancers at *E(spl)*mβ and *E(spl)*m3 at the 8-hour timepoint by ATAC. Neither enhancer exhibited any reduction in accessibility at this timepoint, consistent with the continued recruitment of CSL and the results obtained with MamDN (**Figure 5B**). In contrast, the gradual loss of Mam complexes was accompanied by reduced transcription, as detected by smFISH. Expression of *E(spl)*m3 was already significantly reduced at 4 hours, when levels of nascent transcripts at *E(spl)*-C and of cytoplasmic transcripts had both decreased (Figure S5A). By 8 hours both nascent and cytoplasmic *E(spl)*m3 transcripts were almost undetectable (Figure S5A). Thus, the changes in transcription correlate well with the reduction in Mam

recruitment whereas the chromatin accessibility persists in the absence of Mam. We next investigated whether CSL remained enriched at the locus for an extended period following Notch inactivation. Indeed, we were still able to detect a strong CSL enrichment 24 hours after transfer to the non-permissive temperature at time when, consistent with shorter OFF periods, there was no detectable transcription of *E(spl)*m3 (**Figure 5C**).

One possible consequence of the prolonged CSL enrichment in Notch OFF conditions is that target loci will retain "memory" of previous Notch activation that would make them more receptive to a subsequent exposure to Notch activity. To investigate, we took advantage of the temporal control provided by optogenetic release of NICD using OptIC-Notch{ω} [69]. We compared the response to Notch activation in cells that had been 'preactivated' with blue light for 4 hours and subsequently kept in the dark for 24 hours, and 'naïve' cells, which had been kept solely in the dark and hence had no prior Notch activity (**Figure 5D-F**). We confirmed that cells had no residual transcription after being kept in dark, Notch inactive conditions for 24 hours ("OFF" **Figure 5E**, F). Strikingly, after 30 mins in blue light to activate Notch, cells that had been preactivated showed higher levels of *E(spl)*m3 transcription compared to naïve cells, indicating that the previous Notch exposure renders them more sensitive (**Figure 5E,F**). To investigate whether a previous activation also influences Mam recruitment, we tracked its recovery in a live imaging experiment. As a starting point we deployed a 4 hour Off period, after which Mam was fully depleted at *E(spl)-C* while CSL enrichment remained (**Figure 5G**, H). During the subsequent activation and imaging, recruitment of Mam occurred more rapidly in preactivated cells in comparison to naïve cells, suggesting the former are primed to rapidly reform an active hub containing Mam (**Figure 5I**).

Together, our data indicate that CSL recruitment and increased chromatin accessibility persist after Notch removal and after the loss of Mam-containing activation complexes. This persistent CSL confers a memory state that enables re-assembly of an activation hub and more rapid initiation of transcription in response to subsequent Notch activity.

Probability of transcription conferred by Mastermind

When analysing the smFISH data we noticed that, even in Notch ON conditions, a fraction of nuclei lacked foci of nascent transcription at *E(spl)-C*. Since Mam was present at *E(spl)-C* in all nuclei (**Figure 6A**, S6A), this led us to question whether the presence of Mam-complexes was sufficient to recruit downstream factors required for transcription initiation. We therefore investigated the extent that RNA Pol II was recruited to *E(spl)-C* in Notch ON cells, using endogenous GFP::Rbp3 [16]. When scanning all nuclei, it was evident that Rbp3 enrichment at *E(spl)-C* in Notch ON cells was highly variable. Robust enrichment was detected in a subset of nuclei but, in other cases, there was little/no enrichment above nuclear levels (Figure S6B). Performing a Gaussian population fitting on the data, 2 populations gave the best fit and, based on these, 36% of nuclei had significant enrichment and 64% had similar levels to Notch OFF (**Figure 6B**, S6B). This differs from Mam where all nuclei fall into a single population that has significant Mam enrichment at *E(spl)-C* (**Figure 6A**, S6A). The striking difference in the proportions of nuclei with Pol II and with Mam enrichment implies that there is a limiting step, which results in transcription initiation being probabilistic/stochastic in these conditions.

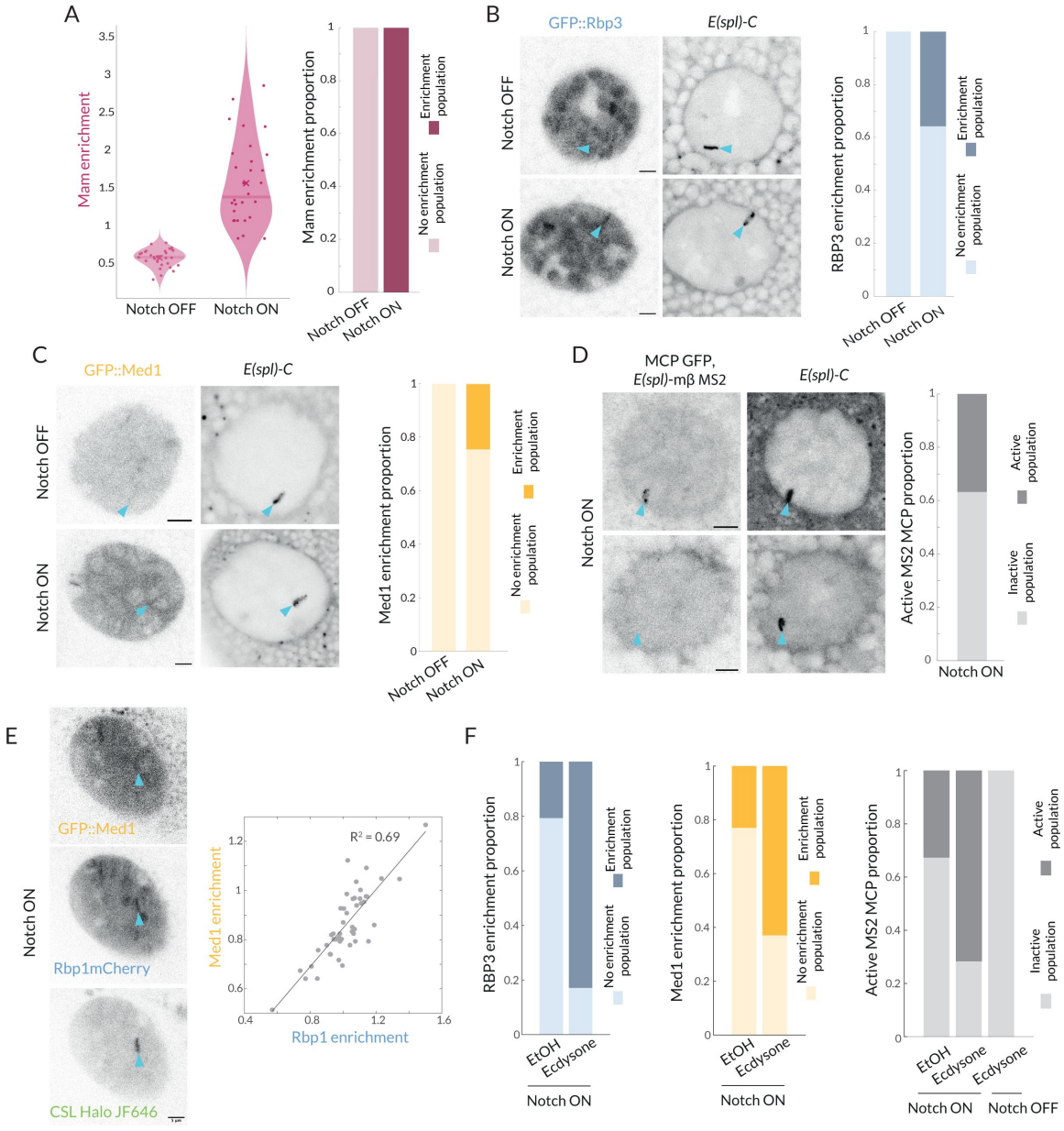
A
Mam enrichment
Notch OFF
Notch ON
Mam enrichment proportion
Enrichment population
No enrichment population
B
GFP::Rbp3
E(spl)-C
Notch OFF
Notch ON
RBP3 enrichment proportion
C
GFP::Med1
Med1 enrichment proportion
D
MCP GFP, E(spl)-mβ MS2
Active MS2 MCP proportion
Active population
Inactive population
E
GFP::Med1
Rbp1mCherry
CSL Halo JF646
R² = 0.69
Med1 enrichment
Rbp1 enrichment
F
EtOH
Ecdysone

Figure 6

Recruitment of Pol II and Med1 in Notch ON is infrequent and is augmented by ecdysone.

(A) GFP::Mam enrichment at *E(spl)-C* in Notch OFF and Notch ON conditions as in **Figure 1**, represented with a violin plot with mean marked by a cross and median by a bar. Right graph: proportions of nuclei with significant enrichment (obtained by performing a Gaussian fit on the fluorescence intensity Images, see Supplementary Figure S5). Over 90% nuclei have significant enrichment (Notch OFF, n = 32, Notch ON, n = 30)

(B) Recruitment of GFP::Rbp3, a subunit of Pol II, at *E(spl)-C* in Notch OFF and Notch ON nuclei. Images: example where enrichment is detected. Graph: proportions of nuclei with significant enrichment as in A (Notch OFF, n = 37, Notch ON, n = 43). All scale bars represent 5um.

(C) Recruitment of GFP::Med1 at *E(spl)-C* in Notch OFF and Notch ON nuclei. Images: example where enrichment is detected. Graph: proportions of nuclei with significant enrichment as in A (Notch OFF and ON, n = 38, 62). All scale bars represent 5um.

(D) Transcriptional activity in Notch ON cells detected using live imaging of GFP::MCP recruited to MS2 loops in transcripts produced by *E(spl)bHLH*mβ (see methods). Images: representative examples of active (upper) and inactive (lower) nuclei. Graph: Proportion of active nuclei (Notch ON, n = 53)

(E) Recruitment of GFP::Med1, mCherry::Rbp1 and Halo::CSL. Med1 and Rbp1 recruitments are correlated. Images: example of co-recruitment of Med1, Rbp1 and CSL. Graph: Correlation plot of max enrichment per nucleus at *E(spl)-C*, (marked by Halo::CSL recruitment), n = 48.

(F) Pretreatment with ecdysone in Notch ON conditions increases proportions of nuclei with recruitment of GFP::Rbp3, GFP::Med1 and with active transcription foci (MS2/MCP intensity) compared to controls (EtOH). Proportions of nuclei with significant enrichment defined as in A. Rbp3 ctrl, ecdysone: n = 39, 36. Med1 ctrl, ecdysone: n = 34, 34. MS2 ON ctrl, ON ecdysone, OFF ecdysone: n = 52, 42, 22.

See also Supplementary Figure S5.

It has been suggested that the core Mediator complex, as distinct from the CDK module, has an important role in bridging between enhancer bound transcription complexes and initiation complexes at promoters [70–72]. To investigate core Mediator recruitment we generated a GFP::Med1 fusion by CRISPR genome-editing. Using this endogenously tagged protein, which is homozygous viable, we found that GFP::Med1 became enriched at *E(spl)-C* with a similar probability to Rbp3 (**Figure 6C**). Indeed when we compared directly the enrichment of Pol II and Med1 in Notch ON nuclei, by using mCherry::Rbp1 [16] to monitor Pol II, we observed a significant correlation between the two proteins (R^2 = 0.69, **Fig 6E**). No such correlation with CSL was observed, in the same experiments (Figures S6E).

To verify that only a subset of nuclei was transcriptionally active we used a strain where MS2 loops have been inserted into *E(spl)*mβ using CRISPR-Cas9 engineering [11] and imaged transcription live in Notch ON nuclei. In the presence of MCP-GFP, which binds to MS2 loops in the RNAs produced, nascent sites of transcription appear as puncta that align into a band of fluorescence at *E(spl)-C*, due to the multiple aligned gene copies. A robust band of MCP/MS2 nascent transcription at *E(spl)-C* was detected in Notch ON conditions, demonstrating that some nuclei were actively transcribing (**Figure 6D**, S6D). However, this was present in only a third (37%) of nuclei. These data show that only a subset of nuclei engage in active transcription, and that the proportion of active nuclei is similar to that with recruitment of Pol II and Med1.

These data demonstrate that presence of Mam-complexes is not sufficient to reliably drive all the steps required for transcription in every Notch ON nucleus. Instead, it appears that transcription is initiated stochastically. Based on previous study in the Drosophila embryo, where transcription in responding nuclei was highly synchronised [73], this probablistic outcome was unexpected although stochastic transcriptional responses have been observed in *C. elegans* [74]. We note that such properties can only be detected using *in vivo* imaging approaches to monitor the responses of individual nuclei, as we have done here.

Ecdysone cooperates with Notch to increase probability of transcription

Even though relatively few Notch ON nuclei became transcriptionally active in our experiments, they all had robust recruitment of Mam complexes and of Med13 at *E(spl)-C*. Thus, in many respects the gene locus becomes competent or poised for transcription in all nuclei. We wondered, therefore, whether the presence of a second stimulatory signal would increase the probability of loci becoming transcriptionally active. In normal development, salivary glands become exposed to the steroid hormone ecdysone a few hours after we perform our experiments. Two observations suggested that ecdysone was a good candidate for a cooperating signal. First, previous genome-wide studies detected ecdysone receptor binding in the *E(spl)-C* region [75]. Second, we noticed in rare samples containing an older gland, that it had a higher proportion of active nuclei. We therefore exposed the early-stage Notch ON salivary glands to ecdysone and analysed the proportion of nuclei with MS2/MCP puncta. Strikingly, the proportion of active nuclei increased dramatically to 70% following ecdysone treatment. No such effects were seen in Notch OFF nuclei where *E(spl)*mβ remained silent even after ecdysone treatment (**Figure 6F**, S6H).

We further tested the effect of ecdysone by measuring changes in enrichment of Pol II and Med1 at *E(spl)-C*. The proportion of nuclei with clear enrichment of each factor was significantly increased (**Figure 6F**, S6F,G). Thus, the switch from the more stochastic transcription elicited by recruitment of Mam alone to the more robust initiation when ecdysone was added, correlated with the presence of Med1 and Pol II. As Mediator is reported to stabilize enhancer-promoter interactions, its recruitment may be what limits the probability of transcription [70,76].

Discussion

Understanding the mechanisms by which signaling levels and dynamics are accurately converted to transcriptional outputs is fundamental for developmental programming. Here we used live imaging approaches to probe how this occurs in the context of the Notch pathway, where the transcriptional relay relies on the single NICD released by each activated receptor and the nuclear complexes it forms with its partners CSL and Mam. By tracking these complexes in real time we unveiled three important features (**Figure 7**): (i) in Notch ON nuclei, the activation complexes promote formation of a dynamic protein hub at a regulated gene locus that concentrates key factors including Mediator CDK module, (ii) the composition of the hub is changeable and the footprint persists after Notch withdrawal conferring a memory that enables rapid reactivation, (iii) transcription is probabilistic in Notch ON nuclei, such that only a third of nuclei with a hub are actively transcribing. This has far-reaching implications because it reveals that stochastic differences in Notch pathway output can arise downstream of receptor activation.

Notch transcription complexes form a hub

Many recent studies have demonstrated that hubs or condensates play key roles in gene-expression regulation by maintaining a high local concentration of transcription factors and other regulatory complexes [17,22,47,70]. By tracking the co-activator Mam in real time, we show

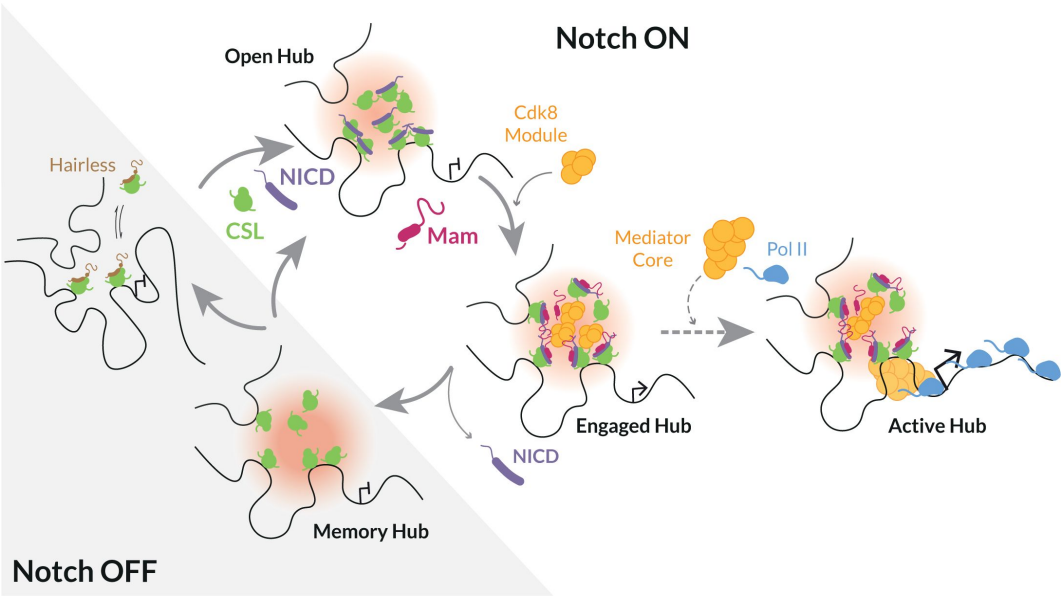

Figure 7.

Model illustrating different modes of Notch transcription-hub.

In the absence of Notch activity (Notch OFF) target genes are inactive, CSL is complexed with co-repressors (e.g. Hairless). Following Notch activation (Notch ON), released NICD (purple) generates a localized high concentration of transcription factors around target enhancer(s) referred to as a "hub" (pink). Open hub: CSL (green) recruitment and accessible chromatin can occur in the absence of Mam. Engaged hub: presence of Mam (magenta) favours recruitment of additional factors, including Mediator CDK8 module (orange). Active hub: productive transcription, transition to this mode, with core Mediator (orange) and Pol II (pale blue) enrichment, is stochastic (dotted arrow). The probability can be enhanced by secondary signal, such as provided by ecdysone. Memory hub: CSL enrichment and chromatin accessibility remain after withdrawal of NICD.

that Notch transcription complexes become enriched around a target locus in a zone that has characteristics of a hub. First, the high-concentration zones are highly dynamic and undergo a continual exchange between activator and repressor complexes. The former exhibit longer residence times, suggesting they are stabilised by other interactions. Second, recruitment of CSL-containing complexes is non-stoichiometric with respect to CSL-binding motifs and can in part be recapitulated by an IDR from NICD. Although deletion of the IDR biases against activation complex recruitment, our evidence suggests that individual IDRs make a minor contribution, as consistent with an unbiased study of IDRs [77]. Third, the enriched zone is readily detectable by live imaging, but is sensitive to fixation, as has been reported for some subcellular protein condensates [46]. Although transcription hubs have frequently been associated with phase separation, examples are emerging where high local concentrations of transcription factors can be achieved without it [21]. Similarly, the locally enriched Notch-induced hubs in our experiments do not manifest clear properties of liquid condensates despite being non-stoichiometric.

We propose that NICD and Mam participate in multivalent interactions which increase the likelihood of the tripartite activation complexes remaining in the chromatin-associated state and which facilitate recruitment of co-activators to form a local hub (**Figure 7**). The latter include subunits of CDK module, Med 13. We find that perturbations to CDK module compromise Mam levels in the hub and vice versa, highlighting its importance. Indeed, the CDK module has been reported to interact directly with Mam and to play a role in Notch signalling output [31,32], and recent studies in mammalian cells indicate CDK8 acts positively in signal-induced gene expression [78]. Although its recruitment is proposed to prepare genes for activation, the transition to activation necessitates CDK8 release, since CDK module sterically inhibits core Mediator-Pol II interactions[76,79]. This is consistent with our results showing that Med13 recruitment is highly dynamic and that, despite most nuclei showing Med13 enrichment within the hub, the probability of transcription is low, as discussed below.

Role of hub in conferring transcriptional memory

Assembly of the transcription hub at *E(spl)-C* depends on Notch activity but, surprisingly, can form in the absence of the co-activator Mam, albeit the composition differs. Notably, CSL complexes continue to be highly enriched and the chromatin at *E(spl)-C* enhancers is accessible in the absence of Mam (**Figure 7**). These properties also persist for many hours after withdrawal of Notch activity and in this way, enhancers that have been switched on by Notch retain an imprint that can influence their response to a subsequent signal, a phenomenon known as transcriptional memory[80,81]. As an indication, after a previous Notch activation event, the conversion to an activation hub with Mam enrichment occurs more rapidly than in the absence of a prior active state and there is enhanced transcriptional activity. Similar accelerated recruitment of STAT1 to promoters occurred in cells with IFNγ-induced transcriptional memory [82], and augmented transcription levels have been seen in several contexts [83,84].

The concept that enhancers retain a memory of a recent Notch signal has several implications. First, naïve and pre-activated loci will respond with different kinetics, which could bias cell-fate decisions when iterative Notch signals are deployed [85]. Second, although our analysis is focused on post-mitotic cells, the footprint may be inherited by daughter cells as CSL is retained on mitotic chromosomes in at least some cell-types [86]. If this is the case, it may explain why enhancer decommissioning is important to switch-off the Notch response in some contexts [87–89]. Third, it could explain some of the observed recruitment of CSL co-repressor complexes to active chromatin if they are involved in sustaining the hub when the signal decays [90,91].

Transcription initiation is probabilistic

Because the *in vivo* live imaging enables us to monitor the responses of individual nuclei, we made the surprising discovery that the presence of Mam-containing hubs at *E(spl)-C* is not sufficient to guarantee transcription. Instead, our results reveal that Mam recruitment confers a 1 in 3 chance

of transcription. As transcription initiation is inherently stochastic [92,93], it is not necessarily unexpected that only a fraction of nuclei would be active at any one time. Indeed, stochastic response to Notch activity has been detected in the *C.elegans* gonad, where a similarly probabilistic response dependent on Notch was detected [74,94]. However this situation differs from the *Drosophila* mesectoderm, where the response to Notch was fully penetrant and highly synchronised across multiple nuclei, arguing that Notch regulated transcription is not a priori stochastic [73]. Furthermore, it has been suggested that recruitment of the activation complex would be the limiting factor. In our context it is evident that recruitment of Mam activation complexes is not the limiting step. This also differs from experiments with the Glucocorticoid receptor, which concluded that it's binding determined the frequency and length of the RNA bursts produced [95].

The observation that at any one time, only a third of nuclei are actively transcribing could be a reflection either of two cell populations, in which only a subset of cells transition to the ON state, or two dynamic states in which all nuclei transition between ON and OFF states. Monitoring transcription live for prolonged periods, we rarely detected transitions in the same nucleus, arguing that, if the differences reflect the dynamic states, both the ON and the OFF state must be of prolonged duration. At the same time, the live traces reveal that the transcription in the ON cells is dynamic, in keeping with frequent fluctuations in promoter states producing "bursts" [92,93]. Thus we would argue that there are two probabilistic steps involved. The first is the transition of the target gene into an active ON state, which, in our basic Notch active condition, appears relatively infrequent, and the second is the switching ON and OFF of the promoter in ON cells to produce "bursts" of RNA, which is much more rapid. The presence of a second signal, in the form of ecdysone was sufficient to increase the probability of the first, slow, transition occurring.

In our experiments, the probability of nuclei being in the ON state correlated with the proportion of nuclei where Med1, a core Mediator subunit, was recruited into the hub at *E(spl)-C*. Mediator is an important intermediary between transcription factors and the preinitiation complex and it functions as an 'integrator' coordinating diverse and combinatorial inputs [70]. The increased probability of Mediator recruitment can thus be explained by an increase in the valency of possible interactions when Notch and ecdysone are both active and present at the enhancers of target genes. We propose that this will be a general mechanism and that other signals/transcription factors will synergise with Notch complexes by adding to the valency of interactions and facilitating recruitment of coactivators to increase the probability of transcription. In different contexts this could toggle the response from one that is stochastic to one that is hard-wired.

The observation of a probabilistic transcriptional outcome downstream of Notch activity and Mam recruitment has profound implications because it has widely been assumed that stochastic differences in Notch pathway output arise due to fluctuations in ligands or ligand availability [96,97]. Our results raise the possibility that differences may also arise due to intrinsic variations subsequent to/independent from receptor activation that affect the probability of transcription occurring. Furthermore, this probability can be modified by other signals, as we observed here with ecdysone, or by the presence of other transcription factors, as when enhancers are 'primed' [73] and/or cooperatively regulated [98–102].

Acknowledgements

We thank Kat Millen and the Genetics Department Fly Facility for performing DNA injections of fly embryos to generate transgenic stocks. We are grateful to Cambridge Advanced Imaging Centre for advice on imaging and to all members of the Bray Lab, for helpful discussions and comments on the manuscript. Stocks obtained from the Bloomington Drosophila Stock Center (NIH P40OD018537) were used in this study.The work was funded by a Wellcome Trust Investigator

Award (212207/Z/18) and an MRC Programme Grant (MR/T014156/1) to SJB. CR and SB were supported by studentships from Wolfson College-University of Cambridge (Dept of Physiology Development and Neuroscience-School of Biological Sciences).

Author contributions

JdeHA, MGL and SJB designed the experiments. JdeHA, SB, JMT performed the experiments. MGL generated critical reagents. JdeHA, CR, SB, JMT and SJB analysed the data. JdeHA and SJB wrote the manuscript, JdeHA, CR, SB, JMT MGL reviewed and commented on the manuscript.

Declaration of interests

The authors declare no competing interests.

Methods

Experimental Animals

Species: *Drosophila melanogaster*. Flies were grown and maintained on food consisting of the following ingredients: Glucose 76g/l, Cornmeal flour 69g/l, Yeast 15g/l, Agar 4.5g/l, Methylparaben 2.5ml/l. Animals of both sexes were used for this study.

Fly Stocks

For genetic manipulations of Notch activity, the Gal4 driver line *1151-Gal4* was combined with *UAS-NΔECD* to provide constitutively active Notch [37,38] or with *UAS-LacZ* as a control. In experiments with fluorescent labelled proteins the following were used: GFP::CSL and GFP::Hairless[34], Halo::CSL, Med13::YFP (BL-57899). Experiments measuring in vivo recruitment to *E(spl)-C* utilized a "locus tag" chromosome in which Int1 sequences had been inserted into an *E(spl)-C* intergenic region and recombined with *UAS-ParB1-mcherry* or *UAS-ParB1-GFP* inserted *AttP.86Fb* [34].

To manipulate protein functions, RNAi lines were as listed in Table S2 and included *UAS-Hairless-RNAi* (Bloomington Drosophila Stock Center, BL-27315), *UAS-Mam-RNAi* (BL-28046), *UAS-Med13-RNAi* (BL-34630), *UAS-nejire-RNAi* (Vienna Drosophila Resource Center, VDRC-102885), *UAS-Cdk8-RNAi* (gifted by [104]) or with *UAS-MamDN* to block Mam activity [67]. Controls as appropriate for each chromosome were *UAS-yellow-RNAi* (II), *UAS-white-RNAi* (III). Crosses were maintained at 25°C and knock-down was validated by RT-qPCR (Figures S1D and S3J).

For temperature manipulations *MS1096-Gal4* (BL-8860) was recombined with *tubulin-Gal80ts* and flies were switched between 29°C non-permissive (Gal80ts inactive, Notch ON) and 18°C permissive (Gal80ts active, Notch OFF) temperatures.

For photomanipulation, transgenes *UAS-Cry2-TevC* and *UAS-OptICNotch{ω}* were recombined onto one chromosome and the conditions used were as described [69] and see below.

For MCP/MS2 live imaging of transcription, a strain in which 24M2 loops were inserted into *E(spl)*mβ-HLH gene was generated by CRISPR using the strategy described [11] details are provided in Table T2. This was combined with *hsp83-MCP::GFP* (BL-7280).

Generation of tagged Mastermind and Med1 flies

CRISPR/cas9 genome engineering was used to introduce fluorescent (sfGFP) or Halo tags into N-terminal coding regions of Mam and Med1 (*flycrispr.org*) to generate seamless protein fusions. Briefly, plasmids for expression of the gRNA (pCFD3-dU6) and for homology arm repair (pHD-ScarlessDsRED) were injected into *nanos-cas9* flies (*flycrispr.org*). Transformants were selected based on the expression of 3xPax3-dsRED which was subsequently removed by crossing to *αTub84B-PiggyBac* flies (BL-32070). Details of gRNA and homology sequences are provided in Table S1.

Generation of flies expressing IDR-GFP fusions

IDR regions of CSL, NICD, Med1 and Mam were isolated from genomic DNA by PCR (Table S1) and inserted into the plasmid pUASt-attB (DGRC, 1419). sfGFP was inserted into the N terminus so that the coding sequences generated an in-frame protein fusion. The resulting plasmids contained an attB sequence and were injected into a strain containing phiC31 integrase and AttP site in position *AttP40* (chromosome II, BL-25709) to obtain transgenic flies for conditional expression of the IDR fusions.

Method Details

Salivary Gland culture and drug/hormonal treatments

Salivary glands were dissected and mounted as described in [34], by submerging mid L3 larvae in M3 Shields and Sang media (Sigma-Aldrich, S3652) supplemented with 5% fetal bovine serum (Sigma-Aldrich, F9665) and 1× Antibiotic-Antimycotic (Gibco,15240-062). For drug and hormonal treatments dissected glands were incubated for an hour with the following compounds: triptolide (10uM, Sigma-Aldrich T3652), Ecdysone (5uM, Cayman Chemicals 16145), A485 (5uM, Cayman Chemicals 24119), Senexin A (1uM, Tocris 4875) and Senexin B (2uM, Cayman Chemicals 24119). After dissection and any treatments glands were mounted into PolyLysine coated coverslips in dissection media supplemented with methyl-cellulose (Sigma-Aldrich, M0387-100G).

Optogenetic Notch activation

The OptIC-Notch{ω} system was used [69]in which blue light conditions induce association of two components, CRY2-TEVc and CIBN-TEVn-mCherry-NICD, which leads to the cleavage and release of NICD, mimicking Notch activation. Larvae were maintained under strict dark conditions and for imaging were dissected under an amber light to maintain OFF conditions. Activation was achieved by transferring larvae to a blue light incubator for the indicated times or by exposure to a blue laser (458 nm) during live-imaging, as described previously [69].

Confocal Imaging and FRAP analysis

Live confocal fluorescence imaging of salivary glands was performed on a Leica SP8 microscope equipped with 7 laser lines (405, 458, 488, 496, 514, 561, and 633) and a 63×/1.4 NA HC PL APO CS2 oil immersion objective and two hybrid GaAsP detectors. Individual nuclei were imaged with a 4.5x zoom, 512×512 pixel resolution, pinhole set to 3-Airy, three line averages, a 12-bit depth and 600 Hz scanning speed. Z-stacks were chosen to encompass the locus and around 9 stacks were acquired. The step size was chosen based on pinhole aperture and was <1um. FRAP was performed on the same microscope but settings were optimised for bleaching and scanning speed: pinhole was opened to 3.5-Airy, speed was increased to 700 Hz, line averaging was removed and Leica FRAP booster was activated. Effective bleaching was achieved by point bleaching. Images before and after bleaching were acquired every 0.4 seconds. After 50 images post bleaching, frame gap was increased to 1 second to minimise unintentional bleaching.

FRAP curves were normalised as described [34], by applying the following:

$$Recovery = \frac{T_{pre} \times B_t}{T_t \times B_{pre}}$$

Where intensities are *Tpre* in a nuclear region before bleaching, *Bt* in the bleached region throughout the experiment, *Tt* in a nuclear region throughout the experiment and *Bpre* the bleached region throughout the experiment.

Single Particle Imaging

Sample preparation and imaging for Single Particle Tracking (SPT) experiments was performed as in [42]. Briefly after dissection glands were incubated with Halo ligand, TMR (Promega, G825A) for 15min and washed in 3 consecutive 10min baths of dissecting medium. Halo ligand concentrations used were 10nM, 10nM, 50nM and 0.01-0.02nM for CSL, Hairless, Mastermind and Histone H2AV respectively. Larvae were imaged on custom build inverted microscope optimised for Single Molecule Localisation Microscopy [34,42] with 50ms exposure time, for 3 to 7min approximately per nuclei.

Immunofluorescence and in situ hybridization

Salivary glands were prepared for immunofluorescence as described previously [34]. Larvae were submerged in PBS and salivary glands were dissected and then fixed in 4% formaldehyde for 15 minutes. Glands were washed three times in PBS + 0.3% Triton X-100. They were later blocked by adding 1% BSA to this buffer. Primary antibody incubation was performed overnight at 4°C with αGFP (1/500, ThermoFisher A6455) and αRFP (1/1000, Chromotek 5F8), αH3K27ac (1/500, ActiveMotif 39135). Glands were washed at least three times with BSA containing buffer, followed by secondary antibody and nuclear stain incubation for two hours at RT (Jackson ImmunoResearch Laboratories, Inc and Sigma). Lastly, they were washed three times and mounted in Vectashield. Image acquisition was performed similarly to live imaging but with a with pinhole closed to 1 Airy and an optimised Z step size, a 0.75 zoom and a 1024×1024 px resolution.

smFISH probes were designed with Stellaris Probe tool for *E(spl)m3-HLH* and salivary glands were processed as described [11]. Briefly, glands were fixed for 45 minutes in 3.7% formaldehyde at RT and permeabilized with overnight in 70% EtOH at 4°C Hybridization and washes were performed according to manufacturer's instructions. Image acquisition was performed similarly to live imaging but with a with pinhole closed to 1 Airy and an optimised Z step size and a 10x zoom. Cytoplasmic images always contained constant Z steps.

ATAC qPCR

Accessibility of genomic regions was probed by tagmentation reaction coupled with qPCR, as described [34]. Briefly, salivary glands were lysed and nuclei were suspended in TD buffer and TD DNA tagment enzyme was added (Illumina #FC-121-1030). The chromatin was tagmented for minutes at 37°C. DNA was amplified with Nextera primers, and samples were normalised by running qPCRs and determining the necessary extra cycles for each sample. Standard qPCRs were performed to quantify accessibility of different regions (primers indicated in Table S1, Roche #04707516001).

RT qPCR

mRNA abundance was measured by retro-transcription coupled with qPCR as described [34]. Briefly, RNA was extracted with Tri Reagent™ (Invitrogen #AM9738), precipitated and DNAse treated (Invitrogen #AM1906). cDNA was generated according to manufacturer's instructions with

M-MLV Reverse Transcriptase (Promega #M1701). Standard qPCRs were performed to measure RNA levels (Roche #04707516001).

Analysis

Confocal image analysis

Images were analysed using MATLAB by importing Leica Images with BioFormat package (MATLAB R2022b, Mathworks & *openmicroscopy.org*). A custom MATLAB app was built to select and rotate the Z stack of interest. A rectangular region of interest of 90×40 pixels was selected for each nucleus, centred on the ParA/B recruitment to IntA/B site in *E(spl)-C* identifiable in one of the channels. Additionally, three circular regions were drawn to measure the nuclear levels in the selected stack, which by division or subtraction enabled normalisation of the rectangular ROI. The ROIs obtained are centred, and this allowed averaging experimental conditions, referred to as "Averaged intensities or enrichment". For the profiles, the ROIs were averaged in the y dimension, and the mean and SEM were represented for each condition. Lastly, for the max enrichment the 10 middle pixels were obtained from the intensity or enrichment profile. In all figures the position of *E(spl)-C* is indicated by a grey bar above Average intensity images and by grey shading/0 in enrichment profile plots.

To obtain proportions of enrichment cells, Gaussian fitting of enrichment values was applied, where the proportion, mean and sigma were used to characterize the enrichment populations. In the correlation, R^2 is the proportion of variance of y explained by the variance of x calculated as 1-RSS/TSS; RSS = sum of squared residuals; TSS = total sum of squares.

SPT analysis

SMLM movies were analysed using the pipeline described in [42]. Localisation of single molecules was carried out using a Gaussian fitting-based approach [105] while a multiple hypothesis tracking algorithm based on [106] was used for tracking. No detection gaps were allowed in tracking except in the case of analyses focusing solely on the duration of trajectories (**Figure 1E**), for which up to 3 detection gaps were allowed. Trajectories consisting of at least 4 time points were then analysed with a Bayesian treatment of HMM, vbSPT [107] and assigned into 2 states, each defined by a Brownian motion diffusion coefficient.

Trajectory density analysis shown in **Fig 1D, E** was carried out by comparing near-locus density with nuclear density using the formula:

$$\frac{No.\,of\ trajectories\ near\ locus}{Total\ no.\,of\ trajectories\ in\ nucleus} \times \frac{Nucleus\ area}{Locus\ area}.$$

Locus and nucleus areas were calculated with standard MATLAB procedures, using the convex hull of localisations and masking.

1-CDF survival curves (**Fig 1E**) were plotted using 99% of trajectories for each molecule, excluding the longest 1% of trajectories which could be artifacts and would have therefore biased our data.

Statistical analysis

N numbers indicate number of nuclei images, unless stated otherwise. If n >30 for both conditions tested, a two tailed t-test was applied. Otherwise, normality was checked via a Shapiro-Wilk test. If both samples were not normal, a Wilcoxon rank sum test was applied. In all cases significance was

presented as follows: * if $p < 0.05$, ** if $p < 0.01$, *** if $p < 0.001$ and **** if $p < 0.0001$ and p-values are provided in Table S4.

References

1. Bray S.J (2016) **Notch signalling in context** *Nat Rev Mol Cell Biol* **17**:722–735 https://doi.org/10.1038/nrm.2016.94

2. Kopan R (2012) **Notch signaling** *Cold Spring Harb Perspect Biol* **4** https://doi.org/10.1101/cshperspect.a011213

3. Borggrefe T., Oswald F (2009) **The Notch signaling pathway: Transcriptional regulation at Notch target genes** *Cellular and Molecular Life Sciences* **66**:1631–1646 https://doi.org/10.1007/s00018-009-8668-7

4. Kovall R.A., Gebelein B., Sprinzak D., Kopan R (2017) **The Canonical Notch Signaling Pathway: Structural and Biochemical Insights into Shape, Sugar, and Force** *Dev Cell* **41**:228–241 https://doi.org/10.1016/j.devcel.2017.04.001

5. Kopan R., Ilagan, Ma.X.G (2009) **The Canonical Notch Signaling Pathway: Unfolding the Activation Mechanism** *Cell* **137**:216–233 https://doi.org/10.1016/j.cell.2009.03.045

6. Sprinzak D., Blacklow S.C (2021) **Biophysics of Notch Signaling** *Annu Rev Biophys* **50**:157–189 https://doi.org/10.1146/annurev-biophys-101920-082204

7. Oswald F., Kovall R.A (2018) **CSL-Associated Corepressor and Coactivator Complexes** :279–295 https://doi.org/10.1007/978-3-319-89512-3_14

8. Nam Y., Sliz P., Song L., Aster J.C., Blacklow S.C (2006) **Structural Basis for Cooperativity in Recruitment of MAML Coactivators to Notch Transcription Complexes** *Cell* **124**:973–983 https://doi.org/10.1016/j.cell.2005.12.037

9. Wilson J.J., Kovall R.A (2006) **Crystal structure of the CSL-Notch-Mastermind Ternary complex bound to DNA** *Cell* **124**:985–996 https://doi.org/10.1016/j.cell.2006.01.035

10. Bray S.J., Gomez-Lamarca M (2018) **Notch after cleavage** *Curr Opin Cell Biol* **51**:103–109 https://doi.org/10.1016/j.ceb.2017.12.008

11. Boukhatmi H., Martins T., Pillidge Z., Kamenova T., Bray S (2020) **Notch Mediates Inter-tissue Communication to Promote Tumorigenesis** *Current Biology* **30**:1809–1820 https://doi.org/10.1016/j.cub.2020.02.088

12. Ilagan M.X.G., Lim S., Fulbright M., Piwnica-Worms D., Kopan R (2011) **Real-time imaging of Notch activation with a luciferase complementation-based reporter** *Sci Signal* **4** https://doi.org/10.1126/scisignal.2001656

13. Housden B.E., Fu A.Q., Krejci A., Bernard F., Fischer B., Tavaré S., Russell S., Bray S.J (2013) **Transcriptional Dynamics Elicited by a Short Pulse of Notch Activation Involves Feed-Forward Regulation by E(spl)/Hes Genes** *PLoS Genet* **9** https://doi.org/10.1371/journal.pgen.1003162

14. Cramer P (2019) **Organization and regulation of gene transcription** *Nature* **573**:45–54 https://doi.org/10.1038/s41586-019-1517-4

15. Lee T.I., Young R.A (2013) **Transcriptional Regulation and Its Misregulation in Disease** *Cell* **152**:1237–1251 https://doi.org/10.1016/j.cell.2013.02.014

16. Cho C.Y., Kemp J.P., Duronio R.J., O'Farrell P.H (2022) **Coordinating transcription and replication to mitigate their conflicts in early Drosophila embryos** *Cell Rep* **41** https://doi.org/10.1016/j.celrep.2022.111507

17. Sabari B.R. *et al.* (2018) **Coactivator condensation at super-enhancers links phase separation and gene control** *Science (1979)* https://doi.org/10.1126/science.aar3958

18. Cho W.-K., Spille J.-H., Hecht M., Lee C., Li C., Grube V., Cisse I.I (2018) **Mediator and RNA polymerase II clusters associate in transcription-dependent condensates** *Science (1979)* **361**:412–415 https://doi.org/10.1126/science.aar4199

19. Rippe K., Papantonis A (2022) **Functional organization of RNA polymerase II in nuclear subcompartments** *Curr Opin Cell Biol* **74**:88–96 https://doi.org/10.1016/j.ceb.2022.01.005

20. Brodsky S., Jana T., Mittelman K., Chapal M., Kumar D.K., Carmi M., Barkai N. (2020) **Mol Cell** :459–471 https://doi.org/10.1016/j.molcel.2020.05.032

21. Trojanowski J., Frank L., Rademacher A., Mücke N., Grigaitis P., Rippe K (2022) **Transcription activation is enhanced by multivalent interactions independent of phase separation** *Mol Cell* **82**:1878–1893 https://doi.org/10.1016/j.molcel.2022.04.017

22. Demmerle J., Hao S., Cai D (2023) **Transcriptional condensates and phase separation: condensing information across scales and mechanisms** *Nucleus* **14** https://doi.org/10.1080/19491034.2023.2213551

23. Hnisz D., Shrinivas K., Young R.A., Chakraborty A.K., Sharp P.A (2017) **A Phase Separation Model for Transcriptional Control** *Cell* **169**:13–23 https://doi.org/10.1016/j.cell.2017.02.007

24. Trylinski M., Mazouni K., Schweisguth F (2017) **Intra-lineage Fate Decisions Involve Activation of Notch Receptors Basal to the Midbody in Drosophila Sensory Organ Precursor Cells** *Current Biology* **27**:2239–2247 https://doi.org/10.1016/j.cub.2017.06.030

25. Kitagawa M (2015) **Notch signalling in the nucleus: roles of Mastermind-like (MAML) transcriptional coactivators. J Biochem** https://doi.org/10.1093/jb/mvv123

26. Ribeiro Just, and Wallberg M. (2009) **Transcriptional Mechanisms by the Coregulator MAML1** *Curr Protein Pept Sci* **10**:570–576 https://doi.org/10.2174/138920309789630543

27. Baghdadi M.B., Castel D., Machado L., Fukada S., Birk D.E., Relaix F., Tajbakhsh S., Mourikis P (2018) **Reciprocal signalling by Notch–Collagen V–CALCR retains muscle stem cells in their niche** *Nature* **557**:714–718 https://doi.org/10.1038/s41586-018-0144-9

28. Castel D., Mourikis P., Bartels S.J.J., Brinkman A.B., Tajbakhsh S., Stunnenberg H.G (2013) **Dynamic binding of RBPJ is determined by Notch signaling status** *Genes Dev* **27**:1059–1071 https://doi.org/10.1101/gad.211912.112

29. Rogers J.M., Guo B., Egan E.D., Aster J.C., Adelman K., Blacklow S.C (2020) **MAML1-Dependent Notch-Responsive Genes Exhibit Differing Cofactor Requirements for Transcriptional Activation** *Mol Cell Biol* **40** https://doi.org/10.1128/MCB.00014-20

30. Fryer C.J., Lamar E., Turbachova I., Kintner C., Jones K.A (2002) **Mastermind mediates chromatin-specific transcription and turnover of the notch enhancer complex** *Genes Dev* **16**:1397–1411 https://doi.org/10.1101/gad.991602

31. Fryer C.J., White J.B., Jones K.A (2004) **Mastermind Recruits CycC:CDK8 to Phosphorylate the Notch ICD and Coordinate Activation with Turnover** *Mol Cell* **16**:509–520 https://doi.org/10.1016/j.molcel.2004.10.014

32. Janody F., Treisman J.E (2011) **Requirements for mediator complex subunits distinguish three classes of notch target genes at the Drosophila wing margin** *Developmental Dynamics* **240**:2051–2059 https://doi.org/10.1002/dvdy.22705

33. Wallberg A.E., Pedersen K., Lendahl U., Roeder R.G (2002) **p300 and PCAF Act Cooperatively To Mediate Transcriptional Activation from Chromatin Templates by Notch Intracellular Domains In Vitro** *Mol Cell Biol* **22**:7812–7819 https://doi.org/10.1128/mcb.22.22.7812-7819.2002

34. Gomez-Lamarca M.J. *et al.* (2018) **Activation of the Notch Signaling Pathway In Vivo Elicits Changes in CSL Nuclear Dynamics** *Dev Cell* **44**:611–623 https://doi.org/10.1016/j.devcel.2018.01.020

35. Franz Oswald, Kovall R.A., Borggrefe Tilman B. D., Giaimo (2018) **Molecular Mechanisms of Notch Signaling** :279–295 https://doi.org/10.1007/978-3-319-89512-3_14

36. Petcherski A.G., Kimble J (2000) **Mastermind is a putative activator for Notch** *Current Biology* **10**:R471–R473 https://doi.org/10.1016/S0960-9822(00)00577-7

37. Rebay I., Fehon R.G., Artavanis-Tsakonas S (1993) **Specific truncations of Drosophila Notch define dominant activated and dominant negative forms of the receptor** *Cell* **74**:319–329 https://doi.org/10.1016/0092-8674(93)90423-N

38. Fortini M.E., Rebay I., Caron L.A., Artavanis-Tsakonas S (1993) **An activated Notch receptor blocks cell-fate commitment in the developing Drosophila eye** *Nature* **365**:555–557 https://doi.org/10.1038/365555a0

39. Struhl G., Adachi A (2000) **Requirements for Presenilin-Dependent Cleavage of Notch and Other Transmembrane Proteins** *Mol Cell* **6**:625–636 https://doi.org/10.1016/S1097-2765(00)00061-7

40. Wachsmuth M (2014) **Molecular diffusion and binding analyzed with FRAP** *Protoplasma* **251**:373–382 https://doi.org/10.1007/s00709-013-0604-x

41. Liu H. *et al.* (2018) **Visualizing long-term single-molecule dynamics in vivo by stochastic protein labeling** *Proceedings of the National Academy of Sciences* **115**:343–348 https://doi.org/10.1073/pnas.1713895115

42. Baloul S., Roussos C., Gomez-Lamarca M., Muresan L., Bray S (2023) **Changes in searching behaviour of CSL complexes in Notch active conditions** *prep*

43. Persson F., Lindén M., Unoson C., Elf J (2013) **Extracting intracellular diffusive states and transition rates from single-molecule tracking data** *Nat Methods* **10**:265–269 https://doi.org/10.1038/nmeth.2367

44. Mazza D., Abernathy A., Golob N., Morisaki T., McNally J.G (2012) **A benchmark for chromatin binding measurements in live cells** *Nucleic Acids Res* **40**:e119–e119 https://doi.org/10.1093/nar/gks701

45. Krejčí A., Bray S (2007) **Notch activation stimulates transient and selective binding of Su(H)/CSL to target enhancers** *Genes Dev* **21**:1322–1327 https://doi.org/10.1101/gad.424607

46. Irgen-Gioro S., Yoshida S., Walling V., Chong S (2022) **Fixation can change the appearance of phase separation in living cells** *Elife* **11** https://doi.org/10.7554/eLife.79903

47. Boija A. *et al.* (2018) **Transcription Factors Activate Genes through the Phase-Separation Capacity of Their Activation Domains** *Cell* **175**:1842–1855 https://doi.org/10.1016/j.cell.2018.10.042

48. Sönmezer C., Kleinendorst R., Imanci D., Barzaghi G., Villacorta L., Schübeler D., Benes V., Molina N., Krebs A.R (2021) **Molecular Co-occupancy Identifies Transcription Factor Binding Cooperativity In Vivo** *Mol Cell* **81**:255–267 https://doi.org/10.1016/j.molcel.2020.11.015

49. Tsai A., Alves M.R., Crocker J. (2019) **Multi-enhancer transcriptional hubs confer phenotypic robustness** https://doi.org/10.7554/eLife.45325.001

50. Kuang Y. *et al.* (2021) **Enhancers with cooperative Notch binding sites are more resistant to regulation by the Hairless co-repressor** *PLoS Genet* **17** https://doi.org/10.1371/journal.pgen.1009039

51. Kawasaki K., Fukaya T (2023) **Functional coordination between transcription factor clustering and gene activity** *Mol Cell* **83**:1605–1622 https://doi.org/10.1016/j.molcel.2023.04.018

52. Emenecker R.J., Griffith D., Holehouse A.S **Metapredict V2: An update to metapredict, a fast, accurate, and easy-to-use predictor of consensus disorder and structure** https://doi.org/10.1101/2022.06.06.494887

53. Wu L., Aster J.C., Blacklow S.C., Lake R., Artavanis-Tsakonas S., Griffin J.D (2000) **MAML1, a human homologue of Drosophila Mastermind, is a transcriptional co-activator for NOTCH receptors** *Nat Genet* **26**:484–489 https://doi.org/10.1038/82644

54. Banani S.F., Lee H.O., Hyman A.A., Rosen M.K (2017) **Biomolecular condensates: organizers of cellular biochemistry** *Nat Rev Mol Cell Biol* **18**:285–298 https://doi.org/10.1038/nrm.2017.7

55. Titov D. V. *et al.* (2011) **XPB, a subunit of TFIIH, is a target of the natural product triptolide** *Nat Chem Biol* **7**:182–188 https://doi.org/10.1038/nchembio.522

56. Clark M.D., Kumar G.S., Marcum R., Luo Q., Zhang Y., Radhakrishnan I (2015) **Molecular Basis for the Mechanism of Constitutive CBP/p300 Coactivator Recruitment by CRTC1-MAML2 and Its Implications in cAMP Signaling** *Biochemistry* **54**:5439–5446 https://doi.org/10.1021/acs.biochem.5b00332

57. Oswald F., Täuber B., Dobner T., Bourteele S., Kostezka U., Adler G., Liptay S., Schmid R.M (2001) **p300 Acts as a Transcriptional Coactivator for Mammalian Notch-1** *Mol Cell Biol* **21**:7761–7774 https://doi.org/10.1128/MCB.21.22.7761-7774.2001

58. Lasko L.M. *et al.* (2017) **Discovery of a selective catalytic p300/CBP inhibitor that targets lineage-specific tumours** *Nature* **550**:128–132 https://doi.org/10.1038/nature24028

59. Kuang Y. *et al.* (2020) **Enhancer architecture sensitizes cell specific responses to Notch gene dose via a bind and discard mechanism** *Elife* **9** https://doi.org/10.7554/eLife.53659

60. Dobi K.C., Halfon M.S., Baylies M.K (2014) **Whole-Genome Analysis of Muscle Founder Cells Implicates the Chromatin Regulator Sin3A in Muscle Identity** *Cell Rep* **8**:858–870 https://doi.org/10.1016/j.celrep.2014.07.005

61. Li X. *et al.* (2020) **The Mediator CDK8-Cyclin C complex modulates Dpp signaling in Drosophila by stimulating Mad-dependent transcription** *PLoS Genet* **16** https://doi.org/10.1371/journal.pgen.1008832

62. Roninson I.B., Porter D.C., Wentland M.P. (2016) **Cdk8-cdk19 selective inhibitors and their use in anti-metastatic and chemopreventative methods for cancer**

63. McDermott M.S.J. *et al.* (2017) **Inhibition of CDK8 mediator kinase suppresses estrogen dependent transcription and the growth of estrogen receptor positive breast cancer** *Oncotarget* **8**:12558–12575 https://doi.org/10.18632/oncotarget.14894

64. Poss Z.C., Ebmeier C.C., Odell A.T., Tangpeerachaikul A., Lee T., Pelish H.E., Shair M.D., Dowell R.D., Old W.M., Taatjes D.J (2016) **Identification of Mediator Kinase Substrates in Human Cells using Cortistatin A and Quantitative Phosphoproteomics** *Cell Rep* **15**:436–450 https://doi.org/10.1016/j.celrep.2016.03.030

65. Lye C.M., Naylor H.W., Sanson B (2014) **Subcellular localisations of the CPTI collection of YFP-tagged proteins in Drosophila embryos** *Development* **141**:4006–4017 https://doi.org/10.1242/dev.111310

66. Lowe N. *et al.* (2014) **Analysis of the expression patterns, subcellular localisations and interaction partners of Drosophila proteins using a pigP protein trap library** *Development* **141**:3994–4005 https://doi.org/10.1242/dev.111054

67. Helms W., Lee H., Ammerman M., Parks A.L., Muskavitch M.A.T., Yedvobnick B (1999) **Engineered Truncations in the Drosophila Mastermind Protein Disrupt Notch Pathway Function** *Dev Biol* **215**:358–374 https://doi.org/10.1006/dbio.1999.9477

68. Giaimo B.D., Oswald F., Borggrefe T (2017) **Dynamic chromatin regulation at Notch target genes** *Transcription* **8**:61–66 https://doi.org/10.1080/21541264.2016.1265702

69. Townson J.M., Gomez-Lamarca M.J., Santa Cruz Mateos C., Bray S.J. (2023) **OptIC-Notch reveals mechanism that regulates receptor interactions with CSL** *Development* **150** https://doi.org/10.1242/dev.201785

70. Richter W.F., Nayak S., Iwasa J., Taatjes D.J (2022) **The Mediator complex as a master regulator of transcription by RNA polymerase II** *Nat Rev Mol Cell Biol* **23**:732–749 https://doi.org/10.1038/s41580-022-00498-3

71. El Khattabi L. *et al.* (2019) **A Pliable Mediator Acts as a Functional Rather Than an Architectural Bridge between Promoters and Enhancers** *Cell* **178**:1145–1158 https://doi.org/10.1016/j.cell.2019.07.011

72. Soutourina J (2018) **Transcription regulation by the Mediator complex** *Nat Rev Mol Cell Biol* **19**:262–274 https://doi.org/10.1038/nrm.2017.115

73. Falo-Sanjuan J., Lammers N.C., Garcia H.G., Bray S.J (2019) **Enhancer Priming Enables Fast and Sustained Transcriptional Responses to Notch Signaling** *Dev Cell* **50**:411–425 https://doi.org/10.1016/j.devcel.2019.07.002

74. Lee C.H., Shin H., Kimble J (2019) **Dynamics of Notch-Dependent Transcriptional Bursting in Its Native Context** *Dev Cell* **50**:426–435 https://doi.org/10.1016/j.devcel.2019.07.001

75. Uyehara C.M., Leatham-Jensen M., McKay D.J (2022) **Opportunistic binding of EcR to open chromatin drives tissue-specific developmental responses** *Proceedings of the National Academy of Sciences* **119** https://doi.org/10.1073/pnas.2208935119

76. Luyties O., Taatjes D.J (2022) **The Mediator kinase module: an interface between cell signaling and transcription** *Trends Biochem Sci* **47**:314–327 https://doi.org/10.1016/j.tibs.2022.01.002

77. Hannon C.E., Eisen M.B. (2023) **Intrinsic protein disorder is insufficient to drive subnuclear clustering in embryonic transcription factors** https://doi.org/10.1101/2023.03.27.534457

78. Chen M. *et al.* (2023) **CDK8 and CDK19: positive regulators of signal-induced transcription and negative regulators of Mediator complex proteins** *Nucleic Acids Res* https://doi.org/10.1093/nar/gkad538

79. Osman S., Mohammad E., Lidschreiber M., Stuetzer A., Bazsó F.L., Maier K.C., Urlaub H., Cramer P (2021) **The Cdk8 kinase module regulates interaction of the mediator complex with RNA polymerase II** *Journal of Biological Chemistry* **296** https://doi.org/10.1016/j.jbc.2021.100734

80. Bonifer C., Cockerill P.N (2017) **Chromatin priming of genes in development: Concepts, mechanisms and consequences** *Exp Hematol* **49**:1–8 https://doi.org/10.1016/j.exphem.2017.01.003

81. Avramova Z (2015) **Transcriptional "memory" of a stress: Transient chromatin and memory (epigenetic) marks at stress-response genes** *Plant Journal* **83**:149–159 https://doi.org/10.1111/tpj.12832

82. Tehrani S.S., Mikulski P., Abdul-Zani I., Mata J.F., Siwek W., Jansen L.E. (2023) **STAT1 is required to establish but not maintain interferon-γ-induced transcriptional memory** *EMBO J* https://doi.org/10.15252/embj.2022112259

83. Ferraro T., Esposito E., Mancini L., Ng S., Lucas T., Coppey M., Dostatni N., Walczak A.M., Levine M., Lagha M (2016) **Transcriptional Memory in the Drosophila Embryo** *Current Biology* **26**:212–218 https://doi.org/10.1016/j.cub.2015.11.058

84. Zhao Z., Zhang Z., Li J., Dong Q., Xiong J., Li Y., Lan M., Li G., Zhu B (2020) **Sustained TNF-α stimulation leads to transcriptional memory that greatly enhances signal sensitivity and robustness** *Elife* **9** https://doi.org/10.7554/eLife.61965

85. Pourquié O. (2003) **The Segmentation Clock: Converting Embryonic Time into Spatial Pattern** *Science (1979)* **301**:328–330 https://doi.org/10.1126/science.1085887

86. Dreval K., Lake R.J., Fan H.-Y (2022) **Analyzing the Interaction of RBPJ with Mitotic Chromatin and Its Impact on Transcription Reactivation upon Mitotic Exit** :95–108 https://doi.org/10.1007/978-1-0716-2201-8_9

87. Zacharioudaki E., Sanjuan J.F., Bray S. (2019) **Mi-2/NuRD complex protects stem cell progeny from mitogenic Notch signaling** https://doi.org/10.7554/eLife.41637.001

88. Jacobs C.T., Kejriwal A., Kocha K.M., Jin K.Y., Huang P (2022) **Temporal cell fate determination in the spinal cord is mediated by the duration of Notch signalling** *Dev Biol* **489**:1–13 https://doi.org/10.1016/j.ydbio.2022.05.010

89. Oldershaw R.A., Tew S.R., Russell A.M., Meade K., Hawkins R., McKay T.R., Brennan K.R., Hardingham T.E (2008) **Notch Signaling Through Jagged-1 Is Necessary to Initiate Chondrogenesis in Human Bone Marrow Stromal Cells but Must Be Switched off to Complete Chondrogenesis** *Stem Cells* **26**:666–674 https://doi.org/10.1634/stemcells.2007-0806

90. Oswald F. *et al.* (2016) **A phospho-dependent mechanism involving NCoR and KMT2D controls a permissive chromatin state at Notch target genes** *Nucleic Acids Res* **44**:4703–4720 https://doi.org/10.1093/nar/gkw105

91. Chan S.K.K. *et al.* (2017) **Role of co-repressor genomic landscapes in shaping the Notch response** *PLoS Genet* **13** https://doi.org/10.1371/journal.pgen.1007096

92. Lammers N.C., Kim Y.J., Zhao J., Garcia H.G (2020) **A matter of time: Using dynamics and theory to uncover mechanisms of transcriptional bursting** *Curr Opin Cell Biol* **67**:147–157 https://doi.org/10.1016/j.ceb.2020.08.001

93. Meeussen J.V.W., Lenstra T.L (2024) **Time will tell: comparing timescales to gain insight into transcriptional bursting** *Trends in Genetics* https://doi.org/10.1016/j.tig.2023.11.003

94. Lee C., Sorensen E.B., Lynch T.R., Kimble J (2016) **C. elegans GLP-1/Notch activates transcription in a probability gradient across the germline stem cell pool** *Elife* **5** https://doi.org/10.7554/eLife.18370

95. Stavreva D.A. *et al.* (2019) **Transcriptional Bursting and Co-bursting Regulation by Steroid Hormone Release Pattern and Transcription Factor Mobility** *Mol Cell* **75**:1161–1177 https://doi.org/10.1016/j.molcel.2019.06.042

96. Nandagopal N., Santat L.A., LeBon L., Sprinzak D., Bronner M.E., Elowitz M.B (2018) **Dynamic Ligand Discrimination in the Notch Signaling Pathway** *Cell* **172**:869–880 https://doi.org/10.1016/j.cell.2018.01.002

97. Kageyama R., Ohtsuka T., Shimojo H., Imayoshi I (2008) **Dynamic Notch signaling in neural progenitor cells and a revised view of lateral inhibition** *Nat Neurosci* **11**:1247–1251 https://doi.org/10.1038/nn.2208

98. Drier Y. *et al.* (2016) **An oncogenic MYB feedback loop drives alternate cell fates in adenoid cystic carcinoma** *Nat Genet* **48**:265–272 https://doi.org/10.1038/ng.3502

99. Terriente-Felix A., Li J., Collins S., Mulligan A., Reekie I., Bernard F., Krejci A., Bray S (2013) **Notch cooperates with Lozenge/Runx to lock haemocytes into a differentiation programme** *Development (Cambridge* **140**:926–937 https://doi.org/10.1242/dev.086785

100. Wang H., Zang C., Taing L., Arnett K.L., Wong Y.J., Pear W.S., Blacklow S.C., Liu X.S., Aster J.C (2014) **NOTCH1–RBPJ complexes drive target gene expression through dynamic interactions with superenhancers** *Proceedings of the National Academy of Sciences* **111**:705–710 https://doi.org/10.1073/pnas.1315023111

101. Larrivée B., Prahst C., Gordon E., del Toro R., Mathivet T., Duarte A., Simons M., Eichmann A (2012) **ALK1 Signaling Inhibits Angiogenesis by Cooperating with the Notch Pathway** *Dev Cell* **22**:489–500 https://doi.org/10.1016/j.devcel.2012.02.005

102. Mittal S., Subramanyam D., Dey D., Kumar R. V., Rangarajan A (2009) **Cooperation of Notch and Ras/MAPK signaling pathways in human breast carcinogenesis** *Mol Cancer* **8** https://doi.org/10.1186/1476-4598-8-128

103. Efron B., Tibshirani R.J. (1994) **Efron, B., and Tibshirani, R.J. (1994). An introduction to the bootstrap (CRC press).**

104. Li X. *et al.* (2020) **The Mediator CDK8-Cyclin C complex modulates Dpp signaling in Drosophila by stimulating Mad-dependent transcription** *PLoS Genet* **16** https://doi.org/10.1371/journal.pgen.1008832

105. Ovesný M., Křížek P., Borkovec J., Švindrych Z., Hagen G.M (2014) **ThunderSTORM: a comprehensive ImageJ plug-in for PALM and STORM data analysis and super-resolution imaging** *Bioinformatics* **30**:2389–2390 https://doi.org/10.1093/bioinformatics/btu202

106. Chenouard N., Bloch I., Olivo-Marin J (2013) **Multiple Hypothesis Tracking for Cluttered Biological Image Sequences** *IEEE Trans Pattern Anal Mach Intell* **35**:2736–3750 https://doi.org/10.1109/TPAMI.2013.97

107. Persson F., Lindén M., Unoson C., Elf J (2013) **Extracting intracellular diffusive states and transition rates from single-molecule tracking data** *Nat Methods* **10**:265–269 https://doi.org/10.1038/nmeth.2367

108. Lobo-Pecellín M., Marín-Menguiano M., González-Reyes A (2019) **mastermind regulates niche ageing independently of the Notch pathway in the Drosophila ovary** *Open Biol* **9** https://doi.org/10.1098/rsob.190127

109. Jia D., Bryant J., Jevitt A., Calvin G., Deng W.-M (2016) **The Ecdysone and Notch Pathways Synergistically Regulate Cut at the Dorsal–Ventral Boundary in Drosophila Wing Discs** *Journal of Genetics and Genomics* **43**:179–186 https://doi.org/10.1016/j.jgg.2016.03.002

110. Ren M. *et al.* (2022) **MED13 and glycolysis are conserved modifiers of α-synuclein-associated neurodegeneration** *Cell Rep* **41** https://doi.org/10.1016/j.celrep.2022.111852

111. Li X. *et al.* (2020) **The Mediator CDK8-Cyclin C complex modulates Dpp signaling in Drosophila by stimulating Mad-dependent transcription** *PLoS Genet* **16** https://doi.org/10.1371/journal.pgen.1008832

Article and author information

F Javier deHaro-Arbona

Department of Physiology Development and Neuroscience University of Cambridge, Downing Street, Cambridge, CB2 3DY, UK

Charalambos Roussos

Department of Physiology Development and Neuroscience University of Cambridge, Downing Street, Cambridge, CB2 3DY, UK

Sarah Baloul
Department of Physiology Development and Neuroscience University of Cambridge, Downing Street, Cambridge, CB2 3DY, UK

Jonathan Townson
Department of Physiology Development and Neuroscience University of Cambridge, Downing Street, Cambridge, CB2 3DY, UK
ORCID iD: 0000-0002-5145-5289

Maria J. Gomez-Lamarca
Department of Physiology Development and Neuroscience University of Cambridge, Downing Street, Cambridge, CB2 3DY, UK, Instituto de Biomedicina de Sevilla (IBiS), Hospital Universitario Virgen del Rocío/CSIC/Universidad de Sevilla, Departamento de Biología Celular, 41013 Seville, Spain

Sarah Bray
Department of Physiology Development and Neuroscience University of Cambridge, Downing Street, Cambridge, CB2 3DY, UK
For correspondence: sjb32@cam.ac.uk
ORCID iD: 0000-0002-1642-599X

Copyright

© 2023, deHaro-Arbona et al.

This article is distributed under the terms of the Creative Commons Attribution License, which permits unrestricted use and redistribution provided that the original author and source are credited.

Editors

Reviewing Editor
Sofia Araújo
University of Barcelona, Barcelona, Spain

Senior Editor
Sofia Araújo
University of Barcelona, Barcelona, Spain

Reviewer #2 (Public Review):

The manuscript from deHaro-Arbona et al, entitled "Dynamic modes of Notch transcription hubs conferring memory and stochastic activation revealed by live imaging the co-activator Mastermind", uses single molecule microscopy imaging in live tissues to understand the dynamics and molecular determinants of transcription factor recruitment to the E(spl)-C locus in Drosophila salivary gland cells under Notch-ON and -OFF conditions. Previous studies have identified the major players that are involved in transcription regulation in the Notch pathway, as well as the importance of general transcriptional coregulators, such as CBP/P300 and the Mediator CDK module, but the detailed steps and dynamics involved in these processes are poorly defined. The authors present a wealth of single molecule data that provides significant insights into Notch pathway activation, including:

(1) Activation complexes, containing CSL and Mam, have slower dynamics than the repressor complexes, containing CSL and Hairless.
(2) Contribution of CSL, NICD, and Mam IDRs to recruitment.
(3) CSL-Mam slow-diffusing complexes are recruited and form a hub of high protein concentrations around the target locus in Notch-ON conditions.
(4) Mam recruitment is not dependent on transcription initiation or RNA production.
(5) CBP/P300 or its associated HAT activity is not required for Mam recruitment
(6) Mediator CDK module and CDK8 activity is required for Mam recruitment, and vice-versa, but not CSL recruitment.
(7) Mam is not required for chromatin accessibility but is dependent on CSL and NICD.
(8) CSL recruitment and increased chromatin accessibility persist after NICD removal and loss of Mam, which confers a memory state that enables rapid re-activation in response to subsequent Notch activation
(9) Differences in the proportions of nuclei with both Pol II and with Mam enrichment, which results in transcription being probabilistic/stochastic. These data demonstrate that presence of Mam-complexes is not sufficient to drive all the steps required for transcription in every Notch-ON nucleus.
(10) The switch from more stochastic to robust transcription initiation was elicited when ecdysone was added.

Overall, the manuscript is well written, concise, and clear, and makes significant contributions to the Notch field, which are also important for a general understanding of transcription factor regulation and behavior in the nucleus. The authors have satisfactorily addressed all my criticisms of their initial submission and therefore congratulate the authors on an excellent paper.

https://doi.org/10.7554/eLife.92083.2.sa1

Reviewer #3 (Public Review):

Summary:

DeHaro-Arbona and colleagues investigate the in vivo dynamics of Notch-dependent transcriptional activation with a focus on the role of the Mastermind (MAM) transcriptional co-activator. They use GFP and HALO-tagged versions of the CSL DNA-binding protein and MAM to visualize the complex, and Int/ParB to visualize the site of Notch-dependent E(Spl)-C transcription. They make several conclusions. First, MAM accumulates at E(Spl)-C when Notch signaling is active, just like CSL. Second, MAM recruits the CDK module of Mediator but does not initiate chromatin accessibility. Third, after signaling is turned off, MAM leaves the site quickly but CSL and chromatin accessibility are retained. Fourth, RNA pol II recruitment, Mediator recruitment and active transcription were similar and stochastic. Fifth, ecdysone enhance the probability of transcriptional initiation.

Strengths:

The conclusions are well supported by multiple lines of extensive data that is carefully executed and controlled. A major strength is the strategic combination of Drosophila genetics, imaging and quantitative analyses to conduct compelling and easily interpretable experiments. A second major strength is the focus on MAM to gain insights into dynamics of transcriptional activation specifically.

Weaknesses:

Weaknesses were minor. and have been addressed in the revised manuscript.

https://doi.org/10.7554/eLife.92083.2.sa0

Author Response

The following is the authors' response to the original reviews.

> ***Public Reviews:***
>
> ***Reviewer #1 (Public Review):***
>
> *In this manuscript by DeHaro-Arbona et al., the authors wish to understand how a signaling pathway (Notch) is dynamically decoded to elicit a specific transcriptional output. In particular, they investigate the kinetic properties of Notch-responsive nuclear complexes (the DNA binding factor CSL and its co-activator Mastermind (mam) along with several candidate interacting partners). Their experimental model is the polytene chromosome of the Drosophila salivary gland, in which the naturally inactive Notch can be artificially induced through the expression of a constitutively active form of Notch.*
>
> *The authors develop a series of CRISPR and transgenic lines enabling the live imaging of these complexes at a specific locus and in various backgrounds (genetic perturbations/drug treatments). This quantitative live imaging data suggests that Notch nuclear complexes form hubs, and the authors characterize their binding dynamics. Interestingly, they elegantly demonstrate that the content of these hubs and their kinetic properties can evolve, even within Notch ON cells. Hence, they propose the existence of distinct hubs, distinguishing an open (CSL), engaged (CSK-Mam), or active (CSL-Mam-Med-PolII) configuration in Notch ON cells and an inactive hub (in Notch OFF having previously been exposed to Notch) state, that would explain the surprising transcriptional memory that the authors observe hours after Notch withdrawal.*

We thank the reviewer for this constructive summary of our work

> ***Reviewer #2 (Public Review):***
>
> *The manuscript from deHaro-Arbona et al, entitled "Dynamic modes of Notch transcription hubs conferring memory and stochastic activation revealed by live imaging the co-activator Mastermind", uses single molecule microscopy imaging in live tissues to understand the dynamics and molecular determinants of transcription factor recruitment to the E(spl)-C locus in Drosophila salivary gland cells under Notch-ON and -OFF conditions. Previous studies have identified the major players that are involved in transcription regulation in the Notch pathway, as well as the importance of general transcriptional coregulators, such as CBP/P300 and the Mediator CDK module, but the detailed steps and dynamics involved in these processes are poorly defined. The authors present a wealth of single molecule data that provides significant insights into Notch pathway activation, including:*
>
> *(1) Activation complexes, containing CSL and Mam, have slower dynamics than the repressor complexes, containing CSL and Hairless.*
>
> *(2) Contribution of CSL, NICD, and Mam IDRs to recruitment.*
>
> *(3) CSL-Mam slow-diffusing complexes are recruited and form a hub of high protein concentrations around the target locus in Notch-ON conditions.*
>
> *(4) Mam recruitment is not dependent on transcription initiation or RNA production.*
>
> *(5) CBP/P300 or its associated HAT activity is not required for Mam recruitment.*

> *(6) Mediator CDK module and CDK8 activity are required for Mam recruitment, and vice-versa, but not CSL recruitment.*
>
> *(7) Mam is not required for chromatin accessibility but is dependent on CSL and NICD.*
>
> *(8) CSL recruitment and increased chromatin accessibility persist after NICD removal and loss of Mam, which confers a memory state that enables rapid re-activation in response to subsequent Notch activation.*
>
> *(9) Differences in the proportions of nuclei with both Pol II and with Mam enrichment, which results in transcription being probabilistic/stochastic. These data demonstrate that the presence of Mamcomplexes is not sufficient to drive all the steps required for transcription in every Notch-ON nucleus.*
>
> *(10) The switch from more stochastic to robust transcription initiation was elicited when ecdysone was added.*
>
> *Overall, the manuscript is well written, concise, and clear, and makes significant contributions to the Notch field, which are also important for a general understanding of transcription factor regulation and behavior in the nucleus. I recommend that the authors address my relatively minor criticisms detailed below.*

We thank the reviewer for their thorough and constructive summary of our work. We are glad that they overall found it insightful and interesting. Below we have addressed the points they have raised.

> *Page 7, bottom. The authors speculate, "It is possible therefore that, once recruited, Mam can be retained at target loci independently of CSL by interactions with other factors so that it resides for longer." Is it possible that another interpretation of that data is that Mam is a limiting factor?*

As indicated our comment is a speculation and is based on the observations summarized in the paragraph. We are not entirely sure what the reviewer is proposing as an alternate model. However, if it relates to the relative concentrations of the different factors, this would not account for the differences in trajectory durations. And for most aspects of our analysis, K[off] has the most profound influence on the results. Furthermore, differences persist even when CSL levels are considerably reduced (as in conditions with Hairless RNAi).

> *Page 9. The authors write, "A very low level of enrichment was evident for… for the CSL Cterminus..". The recruitment of CSL ct IDR does not appear to be statistically significant or there is no apparent difference (Figure S2C), suggesting the CSL ct IDR does not play a role in enrichment.*

We agree with the comments of the reviewer and have adjusted the text on page 9 accordingly.

> *Page 9. The authors write, "Notably, MamnIDR::GFP fusion was present in droplets, suggesting it can self-associate when present in a high local concentration (Figure S2B)." Is this result only valid for Mam nIDR or does full-length Mam also localize into droplets, as has been previously observed for full-length mammalian Maml1 in transfected cells?*

We agree that the observed foci of MamL1 that have been detected in mammalian cells are interesting. We have not tried to replicate those data because the large size of Mam has made it challenging to produce a full-length form in over-expression. We note however that another portion of Mam, MamIDR, does not make droplets when over-expressed despite it

containing a large section of the disordered region of the Drosophila Mam. We have now included a comment about the mammalian data in the text (page 9) to put our findings in context.

> *Previous studies in mammalian cells suggest that Maml1 is a high-confidence target for phosphorylation by CDK8, see Poss et al 2016 Cell Reports https://doi.org/10.1016/j.celrep.2016.03.030. By sequence comparison, does fly Mam have similar potential phosphorylation sites, and might these be critical for Mam/CDK module recruitment?*

We thank the reviewer for highlighting this point. Indeed, we were very excited when we learnt that MamL1 was found to be a high confidence CDK8 target and we looked hard in the Mam sequence for potential phosphorylation sites. Sadly, there is very little conservation between the fly and the mammalian proteins beyond the helical region that contacts CSL and NICD. Furthermore, there are no identifiable putative CDK8 phosphorylation sites based on conventional motifs. It therefore remains to be established whether or not Mam is a direct target of the CDK8 kinase activity. We have added an explanatory comment in the text (page 11).

> *Page 11: The authors write, "The differences in the effects on Mam and CSL imply that the CDK module is specifically involved in retaining Mam in the hub, and that in its absence other CSL complexes "win-out", either because the altered conditions favour them and/or because they are the more abundant." Are the "other" complexes the authors are referring to Hairless-containing complexes? With the reagents the authors have in hand couldn't this be explicitly shown for CSLcomplexes rather than speculated upon?*

The reviewer is correct that CSL complexes containing Hairless are good candidates to be recruited in these conditions. We have compared the levels of Hairless at E(spl)-C following treatments with Senexin and have not detected a difference. However, it appears that the high proportion of unbound Hairless makes it difficult to detect/quantify the enrichment at E(spl)-C. We have therefore taken a different strategy, which is to measure the recruitment of a mutant form of CSL that is compromised for Hairless binding. Recruitment of the mutant CSL is detected in Notch-ON conditions, but is significantly reduced/absent following Senexin treatment. These data favour the model proposed by the reviewer that in the absence of CDK8 activity, the CSL-Hairless complexes win out. These new data have been added in new Supplementary Figure S3F and S3G (and see text page 11)

> *Page 12/13: The authors write, "Based on these results we propose that, after Notch activity decays, the locus remains accessible because when Mam-containing complexes are lost they are replaced by other CSL complexes (e.g. co-repressor complexes)." Again, why not actually test this hypothesis rather than speculate? The dynamics of Hairless complexes following the removal of Notch would be very interesting and build upon previously published results from the Bray lab.*

We thank the reviewer for this comment and we agree it's possible that the proportion of Hairless complexes increases after Notch withdrawal. However, for the reasons outlined above, it is difficult to quantify changes in Hairless, (and our preliminary experiment did not reveal any large-scale effect) and because of the complexity of the genetics we cannot straightforwardly extend the experiment to analyze the behaviour of the mutant CSL as above. Therefore, at present, we cannot say whether the loss of Mam is compensated by an increase in Hairless. We hope in future to investigate the characteristics of the memory in more depth.

> *Page 13: The authors write, "As Notch removal leads to a loss of Mam, but not CSL, from the hub, it should recapitulate the effects of MamDN." While the data in Figure 5B seem*

> *to support this hypothesis, it's not clear to me that the loss of Mam and MamDN should phenocopy each other, bc in the case of MamDN, NICD would still be present.*

We apologise that this sentence was a bit misleading. We have now rewritten it to improve accuracy (page 13) “As Notch removal leads to a loss of Mam, but not CSL, from the hub, we hypothesised it would recapitulate the effects of MamDN on chromatin accessibility and transcription of targets.”

> *The temporal dynamics for Mam recruitment using the temperature- and optogenetic-paradigms are quite different. For example, in the optogenetic time course experiments, the preactivated cells are in the dark for 4 hours, while in the temperature-controlled experiments, there is still considerable enrichment of Mam at 4 hours. For the preactivated optogenetic experiments, how sure are the authors that Mam is completely gone from the locus, and alternatively, can the optogenetic experimental results be replicated in the temperature-controlled assays? My concern is whether the putative "memory" observation is just due to incomplete Mam removal from the previous activation event.*

We appreciate the concerns of the reviewer. However, we are confident that the 4-hour optogenetic inactivation is much more effective than the equivalent time for temperature shifts. The temperature sensitive experiment involves a longer decay, because not only the protein but also the mRNA has to decay to fully remove NICD activity. The optogenetic experiments, involve only protein decay and so are more acute. Furthermore, we have tested (and we show in Figure 5H) that Mam is fully depleted after 4 hours “Off” in the optogenetic experiments.

In order to further strengthen the evidence in favour of the memory hub, we have extended the time-frame further to show that CSL is retained at the locus even after 24 hours “Notch OFF” in both the temperature and the optogenetic paradigm. We have also measured the effects on transcription after a 24hr OFF period using the optogenetic paradigm and seen that robust transcription is initiated in cells that have experienced a previous activation (preactivated) compared to those that have not (naïve). These new data have been added to new Figure 5 C-F and strongly support the memory model.

> ***Reviewer #3 (Public Review):***
>
> *Summary:*
>
> *DeHaro-Arbona and colleagues investigate the in vivo dynamics of Notch-dependent transcriptional activation with a focus on the role of the Mastermind (MAM) transcriptional co-activator. They use GFP and HALO-tagged versions of the CSL DNA-binding protein and MAM to visualize the complex, and Int/ParB to visualize the site of Notch-dependent E(Spl)-C transcription. They make several conclusions. First, MAM accumulates at E(Spl)-C when Notch signaling is active, just like CSL. Second, MAM recruits the CDK module of Mediator but does not initiate chromatin accessibility. Third, after signaling is turned off, MAM leaves the site quickly but CSL and chromatin accessibility are retained. Fourth, RNA pol II recruitment, Mediator recruitment, and active transcription were similar and stochastic. Fifth, ecdysone enhances the probability of transcriptional initiation.*
>
> *Strengths:*
>
> *The conclusions are well supported by multiple lines of extensive data that are carefully executed and controlled. A major strength is the strategic combination of Drosophila genetics, imaging, and quantitative analyses to conduct compelling and easily*

> *interpretable experiments. A second major strength is the focus on MAM to gain insights into the dynamics of transcriptional activation specifically.*

We thank the reviewer for their positive comments about the strengths of our work.

> *Weaknesses:*
>
> *Weaknesses are minor. There were no p-values reported for data presented in Figure S1D and no indication of how variable measurements were. In addition, the discussion of stochasticity was not integrated optimally with relevant literature.*

We thank the reviewer for noting these points. The statistical tests have now been included for Figure S1D (now Figure S1F). We have amplified the discussion about stochasticity, to include more reference to the literature and to make clear also the distinction with transcription bursting (page 19, 20).

> ***Recommendations for the authors:***
>
> ***Reviewer #1 (Recommendations For The Authors):***
>
> *The authors have an elegant series of manipulations that provide strong evidence for their hypotheses and conclusions. Their exploitation of a unique biological system amenable to imaging in the larval salivary gland is well-considered and well-performed. Most of the conclusions are supported by the data. I only have the concerns below.*
>
> *(1) One of the main findings is the composition of Notch nuclear complexes and their interactions within a 'hub'. Yet most of the data showing hubs focus on labeling one protein component (+the locus or transcription), but multi-color imaging is rarely used to show how CSL-Mam, Mam-Med... protein signals coalescence to form a hub. Given the powerful tool developed, it would be important to show these multi-state hubs. Related to this, if the authors expect that hubs are formed independently of transcription or Notch pathway activation, do the authors see clustering at other non-specific loci in the nucleus? If not, can the authors comment on why they think that is the case? If so, do they demonstrate consistent residence time profiles with the tracked E(spl) locus?*

We apologise that it was not evident from the data shown that the proteins co-localize. First we stress that all the experiments are multicolor and most rely on very powerful methods to measure co-recruitment at a chromosomal locus- something that is very rarely achieved by others studying hubs. Second, we have in all cases confirmed that the proteins do colocalize. We have modified the diagram of our analysis pipeline to make more clear that this relies on multi-colour imaging, and adjusted all the figure labels to indicate the position of E(spl)-C. We have also added panels to new supplementary Figure S1C with examples of the co-localization between CSL and Mam and a plot confirming their levels of recruitment are correlated across multiple nuclei.

We would like to clarify that our data show that the hubs do require Notch activation for their establishment. Other regions of enrichment are detected in Notch-ON conditions, but these are less prominent and, with no independent method for identifying them, can't be compared between nuclei. In SPT experiments, other clusters with consistent residence are detected as reported in our recent paper which expanded on the SPT data (Baloul et al, 2023). We also detect co-localizations and "hubs" in other tissues, but those analyses are ongoing and beyond the scope of this paper.

> *(2) The authors convincingly show that Notch hub complexes exhibit a memory. While the data showing rapid hub reformation upon Notch withdrawal are solid and convincing (Figure 5, in particular, F), the claim that this memory fosters rapid transcriptional*

> *reactivation is less clear. Yet in order to invoke transcriptional memory, it's necessary to solidify this transcriptional response angle. The authors should consider quantifying the changes in transcription activity (at the TS and not in the cytoplasm as currently shown), as well as the timing of transcriptional reactivation (with the MS2 system or smFISH). Manipulating the duration of the activation and dark recovery periods could help to draw a better correlation between the timing of hub reformation and that of transcriptional response and would also help determine how persistent this phenomenon is.*

We thank the reviewer for these suggestions. We have carried out several new experiments to probe further the persistence of memory and to show the effects on transcription when Notch is inactivated/reactivated. First, we have extended the time period for Notch inactivation by temperature control and show that the CSL hub persists even at 24 hours and that no transcription from the target E(spl)m3 is detected –neither at the transcription start-site nor in the cytoplasm. Second, we have extended the Notch OFF time period to 24 hours using the optogenetic approach and show that transcription is robustly reinitiated in preactivated nuclei when Notch is re-activated with 30 mins light treatment while little if any E(spl)m3 transcription is detected in naïve nuclei with the same treatment. These new data are included in new Figure 5 C-F and see page 13-14. Both these new experiments substantiate the model that the nuclei retain transcriptional memory.

> *(3) The manuscript ends with the finding that the presence of a Mam hub does not always correlate with transcription. They conclude that transcription is initially stochastic. The authors find this surprising and even state that this could not be observed without their in vivo live imaging approaches. I don't understand why this result is surprising or unexpected, as we now know that transcription is generally a stochastic process and that most (if not all) loci are transcribed in a bursting manner. The fact that E(spl)-C locus is bursty is already obvious from the smFISH data. The fact that active nascent transcription does not correlate with local TF hubs was already observed in early Drosophila embryos (with Zelda hubs and two MS2 reporters, hb-MS2, sna-MS2). If, in spite of the inherent stochasticity of transcription (bursting), the data are surprising for other reasons, the authors should explain it better.*

We apologise that we had not made clear the reasons why the results were unexpected. We have substantially rewritten this section, and the discussion section, to clarify. We have also moderated the language used to better reflect the overall context of our results. We briefly summarise here. As the reviewer correctly states, it is well known that transcription is inherently bursty. Indeed the MS2 transcription profiles in “ON” nuclei are bursty, which likely reflects the switching of the promoter. However, in other contexts where we have monitored transcription although it is bursty it has nevertheless been initiated synchronously in response to Notch in all nuclei in a manner that was fully penetrant. What we observe in our current conditions, is that some nuclei never initiate transcription over the time-course of our experiments (2-3 hours), and those that are ON rarely switch off. This implies that there is another rate-limiting step. Supplying a second signal can modulate this so that it occurs with much higher frequency/penetrance. We consider this to be a second tier of regulation above the fundamental transcriptional bursting.

The fact that Mam is recruited in all nuclei, whether or not they are actively transcribing was surprising because recruitment of the activation complex has been considered as the limiting step. This is somewhat different from Zelda, which is thought to be permissive and needed at an early step to prime genes for later activation rather than to be the last step needed to fire transcription. We note also that we are not monitoring the position of the hub with respect to the promoter, as in the Zelda experiments (Zelda hubs may still persist, but they are not

overlapping with the nascent RNA), we are monitoring the presence or absence of Mam hub in proximity to a genomic region.

> *Minor suggestions:*
>
> *(1) The genotypes of the samples should be indicated in the figure legends.*

We thank the reviewer for this suggestion. We have provided a table (new Table S3) where all of the genetic combinations are provided in detail for each figure. We considered that this approach would be preferable because it would be quite cumbersome to have the genotypes in each legend as they would become very long and repetitive.

> *(2) While the schematic Fig1A explains how the locus is detected, the presence of ParS/ParB is never indicated in subsequent panels and Figure. I assume that all panels depicting enrichment profiles, use a given radius from the ParS/ParB dot to determine the zero of the x-axis (grey zone). This should be clearly stated in all panels/figure legends concerned.*

We apologies if this was not made explicit. Yes, all panels depicting enrichment profiles, use immunofluorescence signal from ParA/ParB recruitment to determine the zero of the x-axis. We have now marked this more clearly In all figures (grey bar, grey shading or labelled 0). All images where the locus is indicated by an arrowhead, by a coloured bar above the intensity plots or by grey shading in the graphs have been captured with dual colour and the signal from ParA/B recruitment used to define its location. This is now clearly stated in the analysis methods and in the legend. We have also modified the diagram in new supplementary Figure S1B, showing our analysis pipeline, to make that more explicit.

> *(3) FRAP/SPT experiments: the author should provide more details. How many traces? Are traces showing bleaching removed?*
>
> *P7: does the statement ' The residences are likely an underestimation because bleaching and other technical limitations also affect track durations' imply that traces showing bleaching have not been removed from the analysis?*
>
> *The authors could justify the choice of the model for fitting FRAP/Spt experiments and be cautious about their interpretation. For example, interpreting a kinetic behavior as a DNA-specific binding event can be accurate, only if backed up with measurements with a mutant version of the DNA binding domain.*

We apologise if some of this information was not evident. The number of trajectories is provided in new Figure S1F, which indicates the number of trajectories analyzed for each condition in Figure 1.

We have now added also the numbers of trajectories analyzed for the ring experiments.

The comments on page 7 about bleaching refer to the technical limitations of the SPT approach. However, as bleached particles cannot be distinguished from those that leave the plane of imaging, they have not been filtered or removed. We have not sought to make claims about absolute residence times for that reason. Rather the point is to make a comparison between the different molecules. As the same fluorescent ligand and imaging conditions are used in all the experiments, all the samples are equivalently affected by bleaching. We subdivide trajectories according to their properties and infer that those which are essentially stationary are bound to chromatin, as is common practice in the field. We note that we have previously shown that a DNA binding mutant of CSL does not produce a hub at E(spl)-C in Notch-ON conditions and has a markedly more rapid recovery in FRAP experiments (Gomez-

Lamarca et al, 2018) consistent with the slow recovery being related to DNA binding. This point has been added to the text (page 8).

> *(4) The authors should quantify their RNAi efficiency for Hairless-RNAi, Med13-RNAi, white-RNAi, yellow-RNAi, CBP-RNAi, and CDK8-RNAi.*

We thank the reviewer for this comment. We have made sure that we are using well validated RNAis in all our experiments and have included the references in Table S2 where they have been used. We have now evaluated the knock-down in the precise conditions used in our experiments by quantitative RT-PCR and added those data, which show efficient knock-down is occurring, to new Supplementary Figure S1D and Figure S3J. We note also that the RNAi experiments are complemented by experiments inhibiting the complexes with specific drugs and that these yield similar results.

> *(5) Figure 3 A: could the author show that transcription is indeed inhibited upon triptolide treatment with smFISH (with for example m3 probes)? Why not use alpha-amanitin?*

We thank the reviewer for this suggestion. We had omitted the smFISH data from this experiment in error. These data have now been added to new Supplementary Figure S3A and clearly show that transcription is inhibited following 1 hour exposure to triptolide. Triptolide is a very fast acting and very efficient inhibitor of transcription that acts at a very early step in transcription initiation. In our experience it is much more efficient than alpha-amanitin and is now the inhibitor of choice in many transcription studies.

> *(6) Figure 4 typo: panel B should be D and vice versa. Accessibility panels are referred to as Figure 4D, D' in the text but presented as panel B in the Figure.*

We thank the reviewer for noting this mistake, it is now changed in the main text.

> *(7) The authors must add their optogenetic manipulation protocol to their methods section.*

The method is described in detail in a recently published paper that reports its design and use. We have now also added a section explaining the paradigm in the methods (Page 31) as requested.

> *(8) Figure 3G needs a Y-axis label.*

Our apologies, this has now been added.

> *(9) The authors should note why there was a change of control in Figure 3D compared to 3E and G (yellow RNAi vs white RNAi).*

This is a pragmatic choice that relates to the chromosomal site of the RNAis being tested. Controls were chosen according to the chromosome that carries the UAS-RNAi: for the second chromosome this was yellow RNAi and for the third white RNAi. This is explained in the methods.

> *(10) Figure 1 would benefit from a diagram describing the genomic structure of the E(spl) locus and the relative position of the labelled locus within it.*

We thank the reviewer for this suggestion and have added a diagram to Supplementary Figure S1A .

> ***Reviewer #2 (Recommendations For The Authors):***
>
> *Minor criticisms and typos:*
>
> *Pet peeve: in some of the figure panels they are labeled Notch ON or OFF, but in others they are not, albeit that info is included in the figure legend. For the ease of the reader/reviewer, would it be possible to label all relevant figure panels either Notch ON or OFF for clarity?*

We thank the reviewer for this suggestion and have modified the figures accordingly.

> *Page 7, top. "In comparison to their average distribution across the nucleus, both CSL and Mam trajectories were significantly enriched in a region of approximately 0.5 μm around the target locus in Notch-ON conditions, reflecting robust Notch dependant recruitment to this gene complex." Are the authors referring to Figure 1D here?*

Thank you, this figure call-out has been added in the text.

> *Page 9. "...reported to interact with p300 and other factors (Figure S2B)." I believe the authors mean Figure S2C and not S2B.*

Thank you, this has been corrected in the text.

> *Page 9. There is no Figure S2D.*

Apologies, this was referring to Figure S1D, and is now corrected in the text.

> *Page 11: "...were at very reduced levels in nuclei co-expressing MamDN (Figure 4B).." Should be Figure 4CD.*

Thank you, this has been corrected in the text.

> *Page 12: "...which was maintained in the presence of MamDN (Figure 4D, D')." Should be Figure 4B.*

Thank you, this has been corrected in the text.

> ***Reviewer #3 (Recommendations For The Authors):***
>
> *In the Results section on Hub, the paragraph starting with "Third, we reasoned . ." the callout to Figure S2D should be Fig S1D.*

Thank you, this has been corrected in the text

> *Figures: The font size in the Figures is so small that most words and numbers cannot be read on a printout. One has to go to the electronic version and increase the size to read it. This reviewer found that inconvenient and often annoying.*

We apologise for this oversight, the font size has now been adjusted on all the graphs etc.

> *Figure legends: the legends are terse and in some cases leave explanations to the imagination (e.g. "px" in Figure 2E). It would be useful to go through them and make sure those who are not a Drosophila Notch person and not a transcription biochemist can make sense of them.*

Our apologies for the lack of clarity in the legends. We have gone over them to make them more accessible and less succinct.